MDPI

Article

Quality Evaluation of Sizeable Surveying-Industry-Produced Terrestrial Laser Scanning Point Clouds That Facilitate Building Information Modeling—A Case Study of Seven Point Clouds

Sander Varbla * , **Raido Puust and Artu Ellmann**

Department of Civil Engineering and Architecture, Tallinn University of Technology, Ehitajate Road 5, 19086 Tallinn, Estonia; raido.puust@taltech.ee (R.P.); artu.ellmann@taltech.ee (A.E.)
* Correspondence: sander.varbla@taltech.ee

Abstract: Terrestrial laser scanning can provide high-quality, detailed point clouds, with state-of-the-art research reporting the potential for sub-centimeter accuracy. However, state-of-the-art research may not represent real-world practices reliably. This study aims to deliver a different perspective through collaboration with the surveying industry, where time constraints and productivity requirements limit the effort which can go to ensuring point cloud quality. Seven sizeable buildings' point clouds (490 to 1392 scanning stations) are evaluated qualitatively and quantitatively. Quantitative evaluations based on independent total station control surveys indicate that sub-centimeter accuracy is achievable for smaller point cloud portions (e.g., a single building story) but caution against such optimism for sizable point clouds of large, multi-story buildings. The control surveys reveal common registration errors around the 5 cm range, resulting from complex surface geometries, as in stairways. Potentially hidden from visual inspection, such systematic errors can cause misalignments between point cloud portions in the compound point cloud structure, which could be detrimental to further applications of the point clouds. The study also evaluates point cloud georeferencing, affirming the resection method's capability of providing high consistency and an accuracy of a few centimeters. Following the study's findings, practical recommendations for terrestrial laser scanning surveys and data processing are formulated.

Keywords: as-built model; error quantification; point cloud; resection method; surveying industry; terrestrial laser scanning (TLS)

1. Introduction

The increasing demand for efficient digital documentation and monitoring of buildings and infrastructure for spatial management, life-cycle planning, maintenance, additional construction installation, and reconstruction requires (i) using building information modeling (BIM) tools and (ii) up-to-date and accurate as-built (in this contribution, as-built is also considered synonymous to as-is) information. The latter, however, is often unavailable or available only partially because as-built geodetic surveys are customarily conducted using conventional surveying methods (e.g., total station and leveling measurements) that provide sparse and subjective point-wise information and are too labor-intensive for mass data collection. It is thus common practice to adopt as-designed construction information instead of as-built digital information to document buildings and infrastructure. Although construction works are conducted according to the as-designed digital models and plans, the actual built geometry can deviate from the design due to stakeout and construction errors, design changes that may remain undocumented, or on-site decisions unforeseen during the planning stage (e.g., pipework placement). Renovations can similarly alter the built geometry from the initial design. Therefore, the as-designed models and plans may not accurately represent the actual building and its components or infrastructure

objects (see the examples in [1–3]). As-built surveys are required to keep the documentation up-to-date and accurate.

Extensive 3D mapping of built geometry can be conducted using emerging methods and technologies (instead of conventional point-wise techniques), such as terrestrial [4–6] and handheld mobile [7–9] laser scanning and drone-based photogrammetry [10–12]. While the accuracy of handheld mobile laser scanning and drone-based photogrammetry is usually estimated around a few centimeters (see the references above), the achievable accuracy of terrestrial laser scanning (TLS)-acquired point clouds is often considered to be at the sub-centimeter level [13–22]. This study focuses on TLS-measured point clouds, since these data are most commonly employed as geometry input for BIM [23]. However, the use of drone technology also has the potential to facilitate sub-centimeter accuracy [24]. A combination of drone-derived and TLS-measured point clouds may, hence, be a preferred strategy for complete coverage of the building or infrastructure object, where drone surveys can provide reliable information for hard-to-reach surfaces [25–27].

Even though the TLS approach can provide high accuracy, point clouds should be evaluated before these data are further utilized. Especially in the cultural heritage domain, intercomparisons between multiple point clouds to assess geometric accuracy [28,29] and point clouds' agreement with pre-defined specifications (both qualitative and quantitative) to evaluate quality compliance to standardized requirements [29] have been pro-posed within the framework of heritage BIM. If point clouds of scanning stations are merged and georeferenced using scanning targets coordinated with a total station survey, the total station established coordinates can also facilitate quality control [30]. However, considering that BIM may require time- and effort-consuming surveys consisting of hundreds of scanning stations, point cloud registration using a cloud-to-cloud-type algorithm (see [5,31,32] and the references therein) is generally employed instead. In such cases, registration uncertainties may significantly influence the accuracy of the resulting compound point cloud, highlighting the need for an independent validation that could reveal errors that may be overlooked otherwise.

Despite the consensus, it must be acknowledged that the accepted sub-centimeter TLS accuracy estimates are usually based on laboratory and simulation studies [13–16] and small-scale investigations consisting of only a few scanning stations [17–21]. Furthermore, these research-based accuracy estimates, which serve as a compelling reference when engaging potential clients and stakeholders, result from meticulous state-of-the-art work. In contrast, time constraints and productivity requirements set significant limitations on the effort to ensure point cloud quality in an industrial setting, all the more as the point cloud validation phase (even the most basic visual inspection) is often neglected. Therefore, detrimental discrepancies between research and what is feasible in a real-world scenario may exist, whereby these discrepancies are often unjustifiably ignored. While TLS is frequently applied in the private sector, no literature (to the best of our knowledge) examines the quality of the produced data. Thus, the primary aim of this study is to provide a different and more realistic point of view (i.e., from a practical standpoint) on the achievable TLS-based point cloud quality through collaboration between researchers and the surveying industry and balance the existing state-of-the-art research results. For this purpose, qualitative and quantitative evaluations of sizable point clouds produced by the surveying industry are conducted, where point cloud errors are quantified using independent total station control surveys.

Another limitation regarding TLS point clouds is that these are often georeferenced in some arbitrary coordinate system (i.e., only the relative positions of scanning targets are required, as in [18,22]) or not georeferenced at all. However, accurate point cloud georeferencing in some regional or national coordinate/height system could be beneficial. For example, Barbarella et al. [17] used an airport's local reference system. Alternatively, Varbla et al. [12,24] georeferenced TLS-acquired point clouds in the Estonian national coordinate and height systems to provide means for validating photogrammetric modeling results derived using an RTK-GNSS (real-time kinematic/global navigation satellite system)

enabled drone. Georeferenced point clouds (and subsequent digital models compiled using such point clouds) can then facilitate cross-utilization of point cloud and BIM datasets with other types of coordinated data, the need for which may arise much later. Thus, the second aim of this study is to assess georeferencing accuracy and consistency (i.e., different surveying companies have surveyed different buildings, whereby the georeferencing of these point clouds must agree within the specified accuracy limits) of sizeable TLS point clouds.

To summarize, this paper evaluates the quality of sizeable TLS point clouds used for BIM. Such a task is crucial because the resulting as-built digital models must accurately represent actual buildings and infrastructure objects, where the modeling directly relies on the quality and integrity of surveyed point clouds. Contrasting with previous studies that have investigated TLS-acquired point clouds, this contribution aims to provide a realistic point of view on the achievable point cloud quality through collaboration with the surveying industry. Such a collaboration interconnects research and real-world use cases and can define new research directions (i.e., industry problems). An overview flowchart of this study can be seen in Figure 1. Accordingly, the remainder of this paper is structured as follows. In Section 2, the examined point clouds are introduced. Sections 3 and 4 then detail the point clouds' qualitative and quantitative evaluations, respectively. The paper ends with a discussion in Section 5 and a brief conclusion in Section 6.
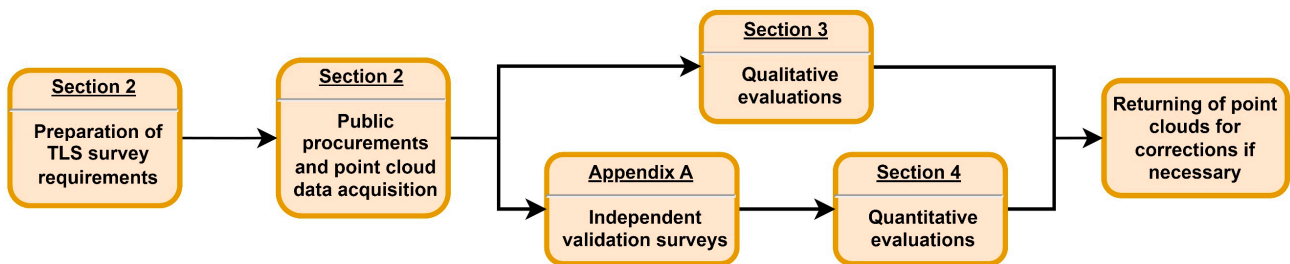

Figure 1. Overview of the experimental process. The headings refer to sections where further details on a specific aspect can be found.

2. The Experiment Setup

This study assesses seven separate TLS-acquired sizeable point cloud datasets surveyed by different teams for varying purposes. These point cloud datasets represent complete coverage (i.e., outdoor and indoor portions merged) of selected buildings within the Tallinn University of Technology campus (located in Tallinn, the capital of Estonia). The first dataset is of the CON building (cf. Figure 2; the building has three above-ground stories and a basement; CON is its official denotation) surveyed for examining deviations of an as-designed digital model from the actual as-built geometry (e.g., up to around 2 dm differences were determined in the placement of some ventilation system details [33]). Point cloud surveys of the CON building were conducted in late 2020 and early 2021, immediately after the CON building reconstruction. Additional survey details will be provided in Section 2.1.

Figure 2. The CON point cloud (also refer to Table 1); the views depict opposite facades.

Table 1. General information of the assessed point clouds.

Point Cloud Identifier	Approximate Area Under a Building	Surveyor	Laser Scanner (cf. Table 2)	Number of TLS Stations (Total Number of Data Points)	Number of Targets Used in Georeferencing	Point Cloud Processing Software
CON (cf. Figure 2)	1610 m² (refer to Figure A1)	Surveyed within the frames of an MSc study [33]	Leica RTC360 LT	490 (1.33 bln [1])	6	Leica Cyclone Core
U02 + U02B	1940 m² (see the shape in Figure 3)	Company 1	Leica RTC360	1130 (0.78 bln)	10	Leica Cyclone Core (version 2022.0.1)
U03 + U03B C1 (cf. Figure 4)	2410 m² (see the shape in Figure 3)	Company 1	Leica RTC360	1392 (1.03 bln)	10	Leica Cyclone Core (version 2022.0.1)
U03 + U03B C3	2410 m² (see the shape in Figure 3)	Company 3	FARO Focus³ᴰ X 330	608 (0.37 bln [1])	4	FARO Scene
U04	1750 m² (see the shape in Figure 3)	Company 2	Leica RTC360	961 (2.54 bln)	8	Leica Cyclone Core (version 2022.0.1)
U05	1750 m² (see the shape in Figure 3)	Company 1	Leica RTC360	1008 (0.79 bln)	10	Leica Cyclone Core (version 2022.0.1)
U06A	1470 m² (see the shape in Figure 3)	Company 2	Leica RTC360	492 (1.42 bln)	28	Leica Cyclone Core (version 2022.0.1)

[1] The number of data points represents both TLS-acquired points and the accompanying points of the roof derived using drone-based photogrammetry; further assessments will be limited to the TLS-acquired portions of point clouds only.

Table 2. Technical specifications of the used terrestrial laser scanners.

Model	Leica RTC360 LT [34]	Leica RTC360 [1] [34]	FARO Focus³ᴰ X 330 [35]
Maximum range	130 m		330 m
Field of view (horizontal/vertical)		360°/300°	
Measurement speed	Up to 1 mln p/s	Up to 2 mln p/s	Up to 0.976 mln p/s
Spatial resolution	Three user-selectable settings: 3, 6, or 12 mm at 10 m		Up to 1.6 mm at 10 m
A priori angular accuracy	18″		Not specified by the manufacturer
A priori range accuracy	1 mm + 10 ppm		2 mm at 10 to 25 m
A priori range precision [2]	0.4 mm at 10 m/0.5 mm at 20 m		0.3 mm at 10 to 25 m
A priori 3D point accuracy	1.9 mm at 10 m/2.9 mm at 20 m/5.3 mm at 40 m		Not specified by the manufacturer
Laser (safety classification/wavelength)		Class 1/1550 nm	
Camera for RGB colored point cloud	A 3-camera system captures a 432 MP 360° × 300° spherical image in one minute		Camera system captures a 70 MP 360° × 300° spherical image

[1] Leica RTC360 also contains a visual-inertial system for automatic point cloud alignment based on real-time tracking of scanner movement between scanner stations; not available for the Leica RTC360 LT version. [2] At 89% (Leica) or 90% (FARO) albedo.
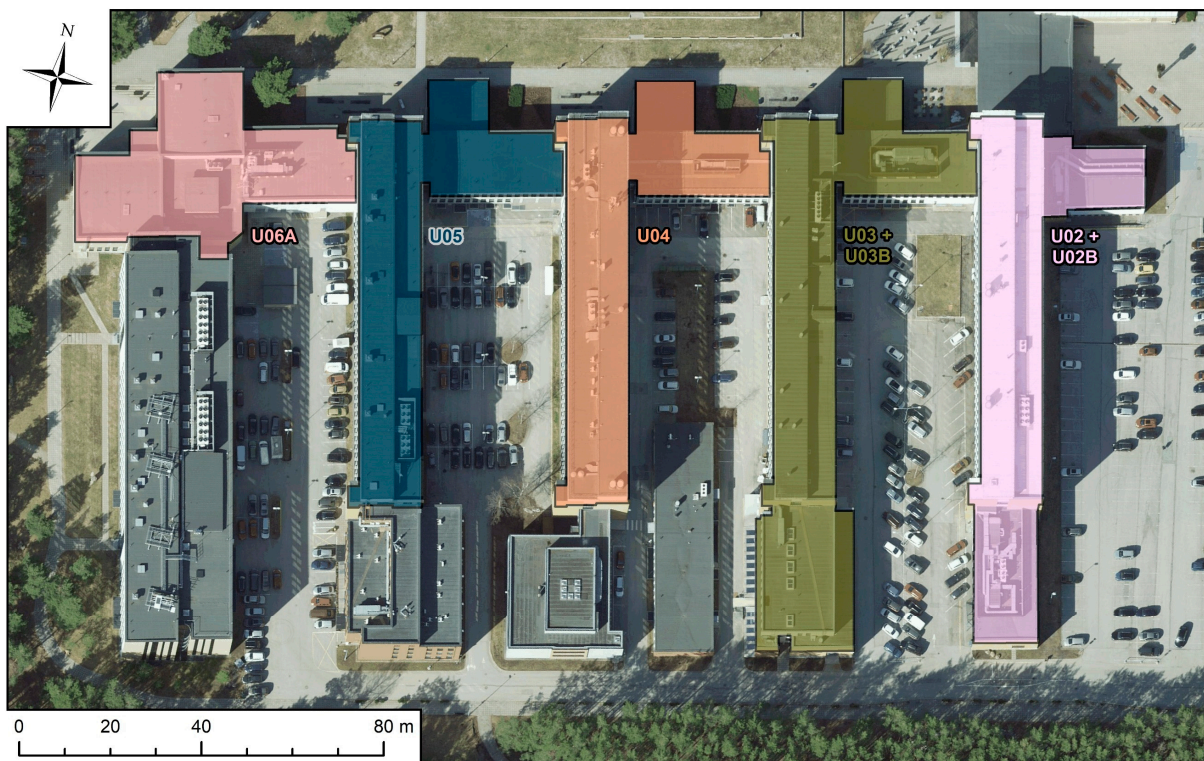
Figure 3. Distribution of TLS surveyed buildings (in color) of the Tallinn University of Technology (also refer to Table 1), assessed within the frames of this study. Background orthophoto originates from the Estonian Land Board.
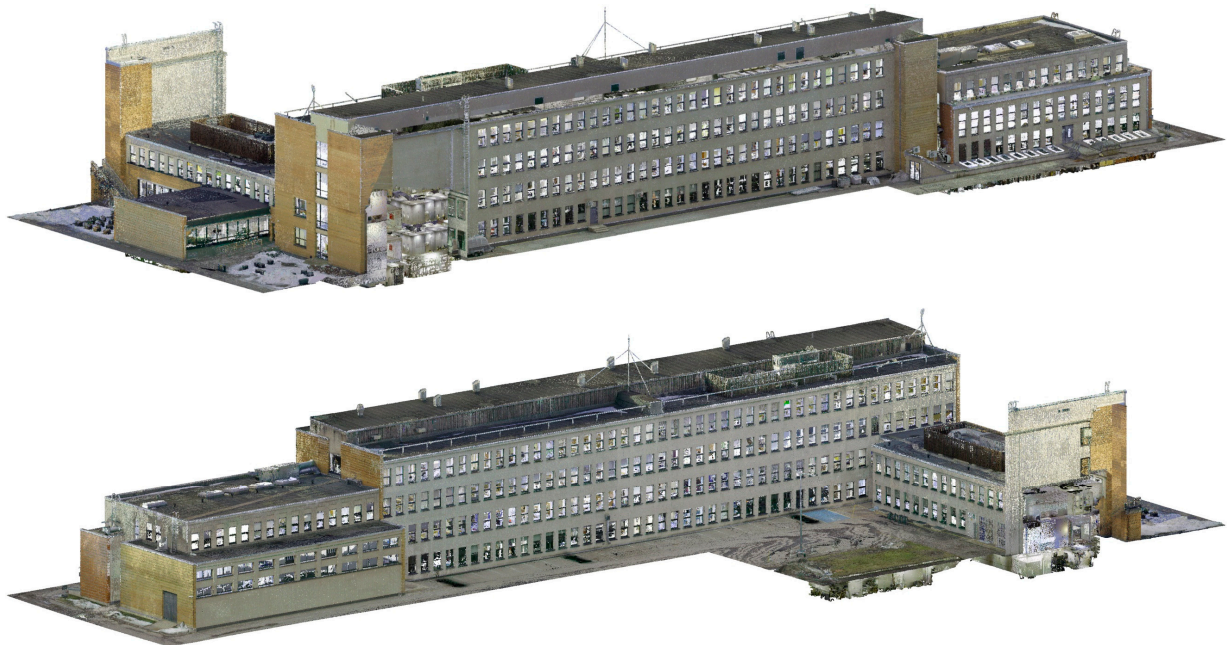

Figure 4. The U03 + U03B C1 point cloud (also refer to Figure 3 and Table 1); the views depict opposite facades.

In 2021, a project was initiated to digitize the entire Tallinn University of Technology campus, employing TLS surveys and BIM. The primary objective was to obtain as-built digital models for developing model-based facility management use cases for the university's real estate office. Most of the campus buildings date back several decades. Back then,

or even during some relatively recent reconstructions dating back just a few years, there were no established BIM (nor surveying) requirements. By understanding the value of up-to-date digital design information for everyday facility management workflows, the project had to define BIM-based design requirements by also considering the availability and quality of as-built data (i.e., existing 2D construction drawings and planned TLS surveys). The requirements were divided based on disciplines (i.e., sub-models). The focus was on how the geometrical models should be constructed in relation to data exchange needs (the CCI classification system was required). Specific modeling rules were defined according to those requirements; sample templates were provided. Note that at this stage, BIM requirements were developed only for the current project. Although some simplifications were defined for this project regarding 3D model content, the developed BIM requirements will be elaborated for future project procurements (design/build). These specific BIM requirements had to be developed, as the contemporary Estonian national BIM requirements (currently in the revision stage) were insufficient for the project's purposes.

On the other hand, TLS requirements were developed to be usable for any future scanning work, too. Therefore, these requirements are rather strict regarding accuracy and spatial resolution. The requirements state that point clouds must have an accuracy of 1 cm (in principle, this embeds the relative positioning of two separate construction elements at opposite ends of a building), both in the horizontal and vertical directions. Following the existing literature (e.g., see the references in the Introduction), it was estimated to be a feasible requirement. The point cloud density requirement was defined as at least 0.5 cm (i.e., the point cloud grid resolution on a measured surface) so that minor building elements would be distinguishable. The selection of scanning stations had to be sufficient to avoid substantial occlusions. The requirements also state that the point cloud georeferencing accuracy must be at least 3 cm relative to the Estonian national L-EST97 rectangular plane coordinate and the EH2000 height systems, respectively. The relative georeferencing accuracy of individual point clouds must remain within 1 cm (i.e., there should be no offsets between point clouds).

Surveying companies, selected via public procurement following the Estonian legislation and Tallinn University of Technology procurement requirements, executed the project-related point cloud surveying and BIM tasks. This study assessed five point cloud datasets, surveyed and processed (in late 2022 and during the first half of 2023) by two companies, henceforth Company 1 and Company 2. Buildings surveyed by Company 1 are U02 + U02B, U03 + U03B (the point cloud associated denotation is C1; cf. Figure 4), and U05; Company 2 surveyed the U04 and U06A buildings. All buildings have five above-ground stories, except U06A—a two-story building; all buildings also have a basement. These buildings' distribution and the corresponding point clouds' extents are shown in Figure 3. Additional survey details will be provided in Section 2.2. Note that buildings under heritage protection, where available building data were most lacking, were surveyed and modeled first—the five assessed point clouds were among those. More campus buildings than indicated in Figure 3 have been surveyed and modeled. However, the current paper has omitted the assessment of those buildings' point clouds, as the five shown in Figure 3 provide sufficient data for envisaging generalized conclusions.

In addition to the previously described point clouds, another earlier surveyed (in early 2021) point cloud of the U03 + U03B building was included in the assessments. The point cloud was surveyed by a surveying company (henceforth Company 3; point cloud associated denotation is C3) for the major reconstruction project of the building. Eventually, the reconstruction was postponed during the preliminary design stage due to some design restrictions for planned construction works; thus, the initial designs had to be redefined. Regardless, the result of a TLS survey was delivered. It should be noted that relatively loose project requirements were imposed for this early survey as the point cloud was only supposed to provide a basis for the reconstruction (not strictly used for a scan-to-BIM workflow as defined in the more recent project). Hence, Company 3's surveyed point

cloud accuracy is expected to be somewhat poorer than the results of Companies 1 and 2. Relevant survey details will be provided in Section 2.3.

General information regarding all seven examined point clouds is summarized in Table 1. Technical specifications of the used laser scanners can be found in Table 2, suggesting that each is sufficient for fulfilling the 1 cm point cloud accuracy requirement im-posed on Companies 1 and 2. Nevertheless, these a priori estimates associated with TLS instruments may be idealized (i.e., characterizing laboratory conditions) and not representative of the actual performance in practice [36]. Various buildings, surveying teams, and equipment, as presented in Tables 1 and 2, can provide means to generalize the results later. However, because point cloud datasets were obtained via project procurements (except the CON building point cloud), the analysis is restricted to the capacity of the selected companies. In other words, the selected methods or used instrumentation and software were offered by the tender; only the earlier described TLS requirements were defined previously. Another limitation of the study is that each building was surveyed only once (except the U03 + U03B building) due to high costs, and consequently, the survey results cannot be compared directly to each other. On the other hand, the main campus buildings (refer to Figure 3) are similar in design and survey conditions, suggesting that similar evaluation results should ideally be expected. The following sub-sections will provide additional details regarding the point cloud surveys that were conducted.

2.1. Surveys of the CON Building

After reconstruction (just before furnishing), TLS surveys were conducted, encompassing the whole CON building, except the roof. Due to time constraints during the initial outdoor TLS survey and due to snowy conditions during the subsequent indoor surveys, the point cloud of the roof was determined using drone-based photogrammetry (since the focus is on TLS, details regarding photogrammetric processing will be omitted). The drone surveys were conducted weekly at the construction site (more details can be found in [12]); the one used here was conducted on the same day as the outdoor TLS survey. The TLS surveys and the subsequent point cloud compilation were performed within the frames of an MSc study [33] supervised by the authors of this paper. At the time, the thesis' author was an industry geodesist with professional experience in point cloud surveying and processing.

A total of 490 scanning stations were required to obtain full point cloud coverage (except the roof) of the CON building. Because the rooms were yet to be furnished, occlusions could be easily avoided. During surveys, the scanning resolution was always set to 12 mm at 10 m (i.e., the sparsest user-selectable scanning resolution; cf. Table 2). Since distances between scanner locations and measured surfaces were generally just a few meters, rarely exceeding 10 m, even the sparsest option was sufficient for a dense and detailed point cloud (all the more, as most surfaces were measured from multiple scanning stations). Images were also captured during the TLS surveys to RGB color the point cloud, which also contains intensity information. Leica Cyclone Core point cloud processing software was used to register surveyed point clouds into a compound point cloud of the building. The point clouds of stations were first aligned visually and then optimized using the software's cloud-to-cloud registration functionality. The cloud-to-cloud registration of Leica Cyclone Core is based on the piecewise (i.e., the registration quality between two point clouds is not affected by the registration of the following point clouds) iterative closest point method [37]. After all TLS surveyed point clouds of stations were registered together, the drone-derived point cloud of the roof was also registered with the rest using Leica Cyclone Core. Figure 2 shows the complete point cloud of the CON building.

Six targets were used to georeference the CON point cloud in the Estonian national L-EST97 rectangular plane coordinate and EH2000 height systems, respectively. Three were standard black-and-white targets taped on the building's wall, and the other three were Leica high-definition surveying targets set up on top of survey nails. The targets were coordinated based on a previously established survey network at the construction

site [12] using a Trimble S6 2″ robotic total station [38] and the resection (i.e., free stationing) method [39–41]. The resection method is a standard technique in surveying that allows for determining total station position coordinates at an arbitrary location (hence free stationing) by measuring distances to points with known coordinates and angles between those points relative to the total station position. The root mean square error (RMSE) estimates of georeferencing residuals between target locations in the point cloud and the total station surveyed targets' coordinates were 0.3 cm for the X-coordinate, 0.4 cm for the Y-coordinate, and 0.6 cm for the height after point cloud transformation, suggesting at least around a centimeter for the georeferencing accuracy (assuming no biases exist in the survey network).

2.2. Surveys Conducted by Companies 1 and 2

During TLS surveys, Companies 1 and 2 varied the scanning resolution between the three user-selectable settings (refer to Table 2) depending on the distance between a scanning station and measured surfaces to ensure dense and detailed point clouds. In addition to point cloud intensity information, Companies 1 and 2 captured the scene images to generate RGB-color data attached to the point clouds. Both companies used Leica Cyclone Core to register surveyed point clouds into compound point clouds. As an example, Figure 4 shows the U03 + U03B C1 point cloud. Table 1 suggests that Company 1 has also decimated the point clouds (compared to Company 2 results) to reduce data size and improve point cloud utilization performance. From qualitative assessments, the point clouds of Company 2 are visually denser, but the results of both companies are sufficiently detailed to (generally) clearly distinguish even the smallest/finest objects (e.g., power sockets, light switches, visible pipework).

Both companies used the resection method to establish (independently) survey networks for coordinating standard black-and-white scanning targets (numbers of targets are presented in Table 1), used for georeferencing the point clouds in the Estonian national L-EST97 rectangular plane coordinate and EH2000 height systems, respectively. Company 1 employed two local geodetic network polygonometry benchmarks (one to the east of the U02 + U02B building and the other to the southeast; refer to Figure 3 for the building location) to establish the base station for the total station survey. Company 2 used the same two polygonometry benchmarks and included a third (located northeast of the U02 + U02B building) to establish the base station of the total station for the survey. All three polygonometry benchmarks are within 200 m of the U02 + U02B building. For the surveys, Company 1 used a Trimble S5 5″ robotic total station [42], and Company 2 used a Leica Viva TS12 3″ robotic total station [43].

2.3. Surveys Conducted by Company 3

Like the CON point cloud, TLS surveys by Company 3 encompassed the whole U03 + U03B building, except the roof. Due to loose accuracy requirements, a drone-based photogrammetric survey was quite acceptable for determining the point cloud portion of the roof. During TLS surveys, grayscale images were captured; hence, only the drone-derived roof portion of the point cloud is RGB-colored. Like all other point clouds, Company 3's surveyed point cloud does contain intensity information. FARO Scene point cloud processing software was used to register surveyed point clouds into a compound point cloud of the U03 + U03B building. Then, the drone-derived point cloud of the roof was also registered with the rest using the FARO Scene. Similarly to Leica Cyclone Core, cloud-to-cloud registration implemented in FARO Scene is also based on the piecewise iterative closest point method [37].

Since high accuracy was not requested for point cloud georeferencing in L-EST97 and EH2000, four points (i.e., some easily distinguishable objects) distributed around the U03 + U03B building were RTK-GNSS measured relative to a commercial network of continuously operating GNSS reference stations using a Sokkia GRX3 GNSS receiver [44]. Ellipsoidal heights were reduced to normal heights (corresponding to the EH2000 system) using the national EST-GEOID2017 [45] quasigeoid model. These GNSS-determined points

were matched with the point cloud to georeference the latter. Compared to all other assessed point clouds, the georeferencing accuracy of the U03 + U03B C3 point cloud is expected to be lower. Thus, this point cloud's assessment focuses more on determining registration errors.

3. Qualitative Evaluation of Point Clouds

For BIM, point clouds:

1. should be complete (i.e., not significantly occluded) to capture all construction details following the required level of detail [6,29,30].
2. should be sufficiently dense, to discern the smallest construction elements following the required level of detail, whereby RGB and intensity information are also beneficial for correctly interpreting a point cloud [28–30].
3. must be registered together correctly (e.g., a construction element in one end of the building has to be accurately located relative to another on the opposite end) to maintain the integrity of the point cloud and its compliance with the surveyed object [1,29].
4. should contain only a little noise (e.g., reflections, people, and other moving objects) to reduce computational load and not hinder the modeling, which is especially important if automated approaches are used [6,46]. The noise can also cause and exacerbate point cloud registration errors [5,31,32].
5. Optionally, the registered compound point cloud ought to be georeferenced accurately relative to some national or regional coordinate/height system to position it relative to other coordinated data [28–30].

Additional details on criteria imposed on TLS point clouds can be found in a review compiled by Aryan et al. [47]. This section will now focus on the apparent quality of point clouds: evaluation of occlusions, noise, and registration discrepancies between point clouds of scanning stations in the compound point cloud.

During the post-survey assessments, it became clear that the apparent quality of point clouds surveyed by Companies 1 and 2 was generally according to expectations. However, some rooms or building sections were significantly occluded (e.g., due to obstacles in a room; an occlusion example is in Figure 5a) or, on a few occasions, not measured (e.g., due to access limitations). In these cases, the initial BIM models were compiled using outdated, archived documentation of corresponding buildings. If possible, such rooms and building sections were requested to be scanned (if it was obvious that occlusions affected modeling quality) and models corrected accordingly. While the CON point cloud contained no remarkable occlusions, the U03 + U03B C3 point cloud was significantly occluded in some parts of the building. One such example is presented in Figure 5b. These occlusions are why fewer points could be used for validating the U03 + U03B C3 point cloud (compared to Company 1 results) in Section 4.
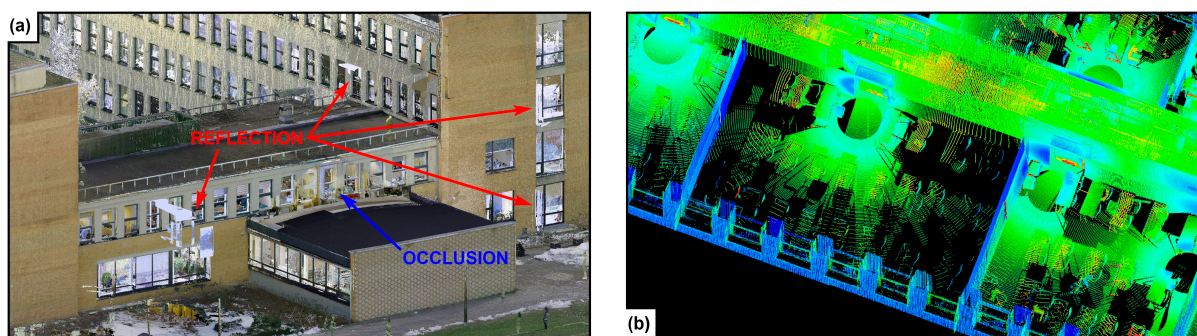

Figure 5. Reflections (red arrows) and an occlusion (blue arrow) in the U04 (refer to Figure 3) point cloud (**a**), and occlusions in the U03 + U03B C3 (refer to Figure 3) point cloud ((**b**); the point cloud is colored according to intensity information—blue denotes high intensity and reddish low).

Regarding noise, all surveyed point clouds contain some reflections (see the example in Figure 5a) and artifacts of passing people to varying levels. Admittedly, it was not specified in the requirements provided to the surveying companies that point clouds must be cleaned (this requirement should be included when updating survey requirements in the future). During the assessments of point clouds surveyed by Companies 1 and 2, it was determined that BIM quality should generally not suffer due to noise as the point cloud details (e.g., in corridors where bypassing people moved) were distinguishable. Most surveys were also conducted when few people were around. The U03 + U03B C3 point cloud is similar to those of Companies 1 and 2 in terms of noise. In contrast, the CON point cloud was cleaned from the most significant reflections. During the survey, only surveyors were present at the CON building; hence, people moving around was not a problem.

In addition to the overall appearance of point clouds, the initial visual inspection also assessed the registration quality. All point clouds were checked carefully for discrepancies between point clouds of scanning stations in a compound point cloud. In the case of the CON point cloud, most discrepancies that could be detected were within a centimeter and generally did not exceed 2 cm. Nevertheless, there were some exceptions. One basement floor corridor wall was an unusual case where discrepancies appeared between point clouds of four scanning stations (cf. Figure 6a); the corresponding difference between extremes reached 3.6 cm. The registration discrepancies usually appear between two distinct groups of point clouds instead. Another more significant discrepancy of around 7 cm could be found in the third-floor wall near a narrow stairway. This stairway-related point cloud registration problem will be further discussed in Section 4.
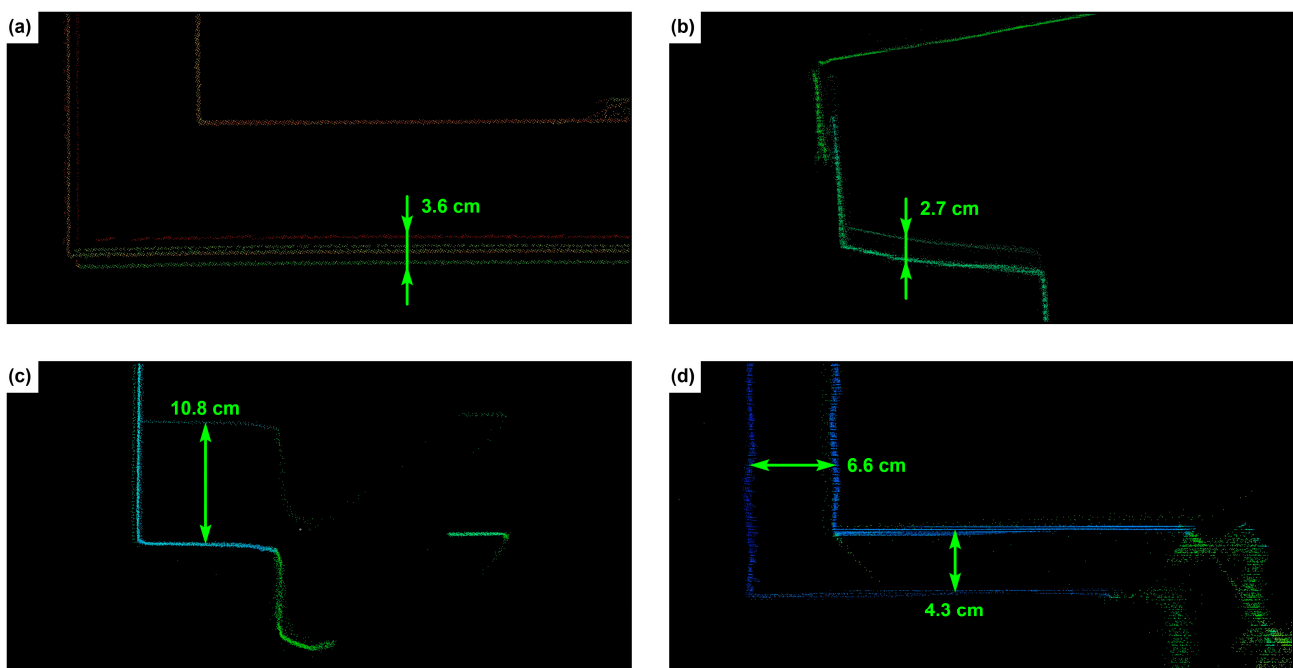

Figure 6. A selection of more significant registration errors in different point clouds: basement floor corridor wall discrepancies (horizontal plane) in the CON point cloud (**a**), vertical discrepancies in the eaves overhang of the U05 (refer to Figure 3) point cloud (**b**), vertical outer wall discrepancies in the U06A (refer to Figure 3) point cloud at a window (**c**), and vertical (4.3 cm) and horizontal (6.6 cm) discrepancies in the U03 + U03B C3 (refer to Figure 3) point cloud at an exterior doorway (**d**). Point clouds are colored according to intensity information—blue denotes high intensity, and the reddish color low.

The examinations of Company 1 and Company 2's results yielded similar conclusions—most discrepancies that could be visually detected were within a centimeter. A few more significant discrepancies, as shown in Figure 6b, were in the 2–3 cm range. One excep-

tional height-wise discrepancy of around a decimeter was found in the U06A point cloud (Figure 6c). However, this discrepancy appeared outside the BIM target area and was thus not considered detrimental to the modeling. Regarding more recent surveys (not included in the assessments of this study), an occasion was found where several rooms of a point cloud had height-wise registration discrepancies exceeding a decimeter. The affected point cloud was requested to be corrected. More significant problems were also found with the U03 + U03B C3 point cloud. Several discrepancies up to 10–15 cm were discovered. An example of a discrepancy in both horizontal and vertical directions is shown in Figure 6d (i.e., a significant misalignment of point cloud portions). Such an erroneous point cloud demonstrates that there must be some inspection arranged from the client's side to determine the quality of the provided point clouds. It should be noted (based on visual inspections) that a common tendency observed between the point clouds surveyed by Companies 1 to 3 was that more significant registration errors were more likely to appear outdoors than inside the buildings. The likely reason is that indoor point cloud registration is more constrained (i.e., point clouds of scanning stations generally contain multiple walls, a floor, and a ceiling) compared to outdoors (i.e., surveyed point clouds generally contain one or two walls and the ground, which may be irregular due to, e.g., vegetation).

4. Quantitative Evaluation of Point Clouds

All validation surveys (i.e., survey network establishment and measuring validation points) of Section 2's described point clouds were conducted using a Trimble S6 2″ robotic total station [38] and the resection method. Computational details for resection establishment using Trimble instruments are explained in [48] (refer to the standard resection). Relevant technical information regarding the total station surveys can be found in Appendix A. Reliable determination of georeferencing errors can be conducted based on the assessments of total station surveys (cf. Appendix A). Furthermore, the total station surveys are sufficiently accurate for investigating the integrity of the point clouds (i.e., determining significant registration errors).

It should be noted that the accuracy of the total station horizontal position using resection depends on the uncertainties associated with the total station measurements and the number and accuracy of existing points employed in the resection establishment, whereby the optimal horizontal location for the total station is in the center of gravity of the used points [40,41]. This principle was followed as much as feasible, unless occasional complex measuring geometry made it impossible. On the other hand, the height component accuracy depends only on the total station measurement uncertainties and the number and accuracy of existing points employed in the resection establishment; the distribution of these points has a negligible influence [41]. Relatedly, the superior accuracy of the vertical coordinate components of the total station surveys is evident from the assessments in Appendix A—millimetric height accuracy can be assumed for the survey networks.

All the examined discrepancies in the following are obtained by subtracting validation points' coordinates, determined by the total station (as described in Appendix A), from those extracted from point clouds; the selection of validation points is explained in Appendix A.1 (see principle number 3). In addition to coordinate discrepancies, baseline discrepancies $D^{Baseline}$ between a point cloud and total station estimated baselines ($PC^{Baseline}$ and $TS^{Baseline}$, respectively) were also computed:

$$
\begin{aligned}
D^{Baseline} &= PC^{Baseline} - TS^{Baseline} \\
&= \sqrt{\left(X_{PC}^A - X_{PC}^B\right)^2 + \left(Y_{PC}^A - Y_{PC}^B\right)^2 + \left(H_{PC}^A - H_{PC}^B\right)^2} \\
&\quad - \sqrt{\left(X_{TS}^A - X_{TS}^B\right)^2 + \left(Y_{TS}^A - Y_{TS}^B\right)^2 + \left(H_{TS}^A - H_{TS}^B\right)^2},
\end{aligned}
\tag{1}
$$

where X, Y, and H are X-coordinate, Y-coordinate, and height, respectively. Superscripts A and B denote an arbitrary point pair, and subscripts PC and TS indicate the point cloud and total station obtained coordinate components. Note that baselines (from a few meters up to around a hundred meters) are only computed between such points that are (likely)

not scanned from the same scanning station (i.e., baselines that formed between nearby points on the same structure or points in the same room were excluded).

4.1. The CON Point Cloud

Descriptive statistics regarding discrepancies between validation points' coordinates and those extracted from the CON point cloud are summarized in Figure 7 (considering all 59 validation points). It can be noticed that the mean discrepancies are 0.5 cm for the *X*-coordinate, −1.7 cm for the *Y*-coordinate, and −0.5 cm for the height. Considering total station survey accuracy (cf. Figure A1), these results suggest proper georeferencing of the point cloud. It should be noted that significant point cloud registration errors also contribute to these mean discrepancies, which will be discussed subsequently.
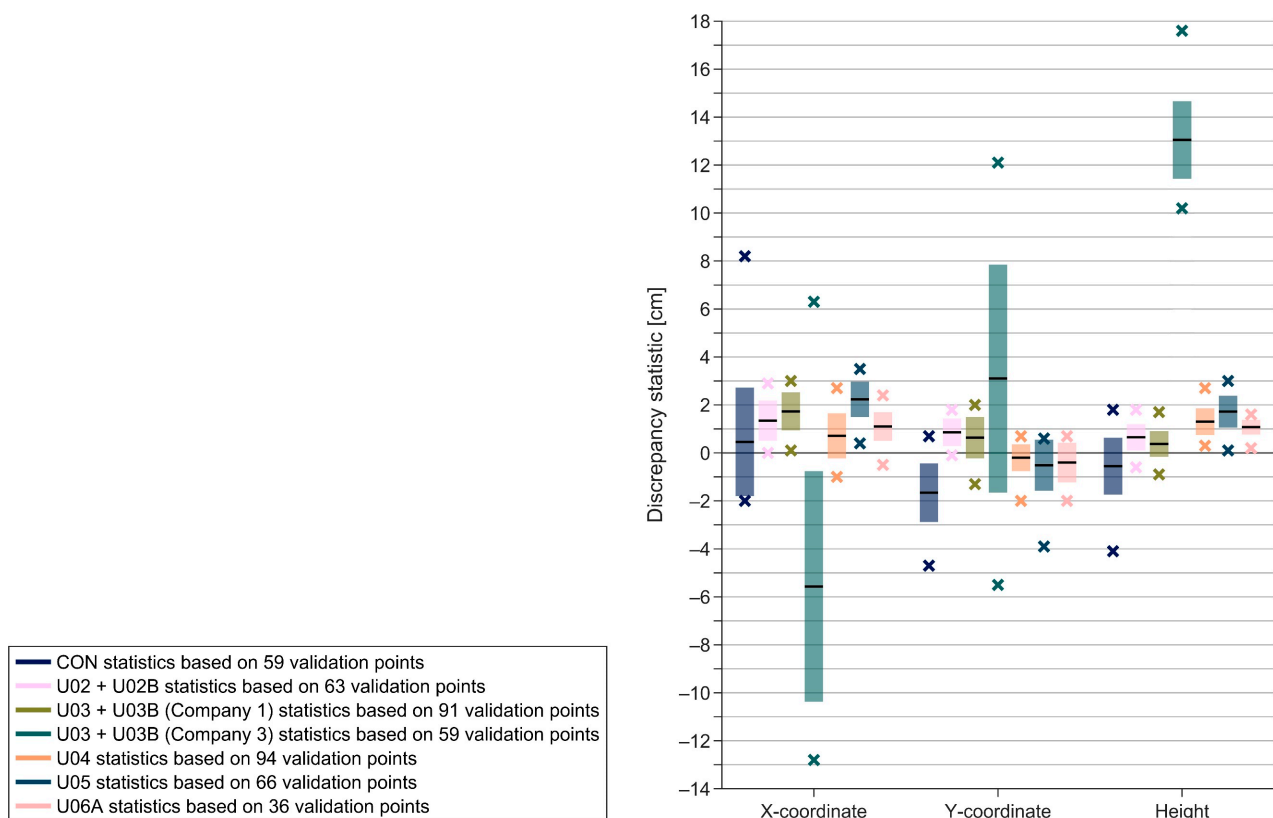

Figure 7. Descriptive statistics of discrepancies between validation points' coordinates and those extracted from point clouds. Black lines denote mean values, colored bars standard deviation estimates, and colored crosses minimum and maximum discrepancies. Note that the CON-associated statistics represent an indoor survey, whereas all others describe outdoor surveys' results.

The standard deviation estimates of 1.2 cm for the *Y*-coordinate and height seem to indicate good consistency between the point cloud and validation survey (cf. Figure 7). In contrast, a standard deviation of 2.3 cm for the *X*-coordinate is more concerning, where the increased value is due to plus-signed discrepancies up to 8.2 cm. Although the baseline discrepancies' (Figure 8) standard deviation estimate of 1.6 cm suggests relatively good consistency, discrepancies up to 7.3 cm also appear. A more detailed comparison of discrepancies based on individual floors (Figure 9) demonstrates that problems occur on the basement (height component) and third (*X*- and *Y*-coordinate components) floors. Consistency between the validation survey and the point cloud is good on the first and second floors, where standard deviation estimates remain within 0.7 cm. Note that significant discrepancies in the ventilation system details, up to around 2 dm between the as-designed digital model and point cloud (interested readers can find these comparisons in [33]), as mentioned in Section 2, were examined on the first floor.
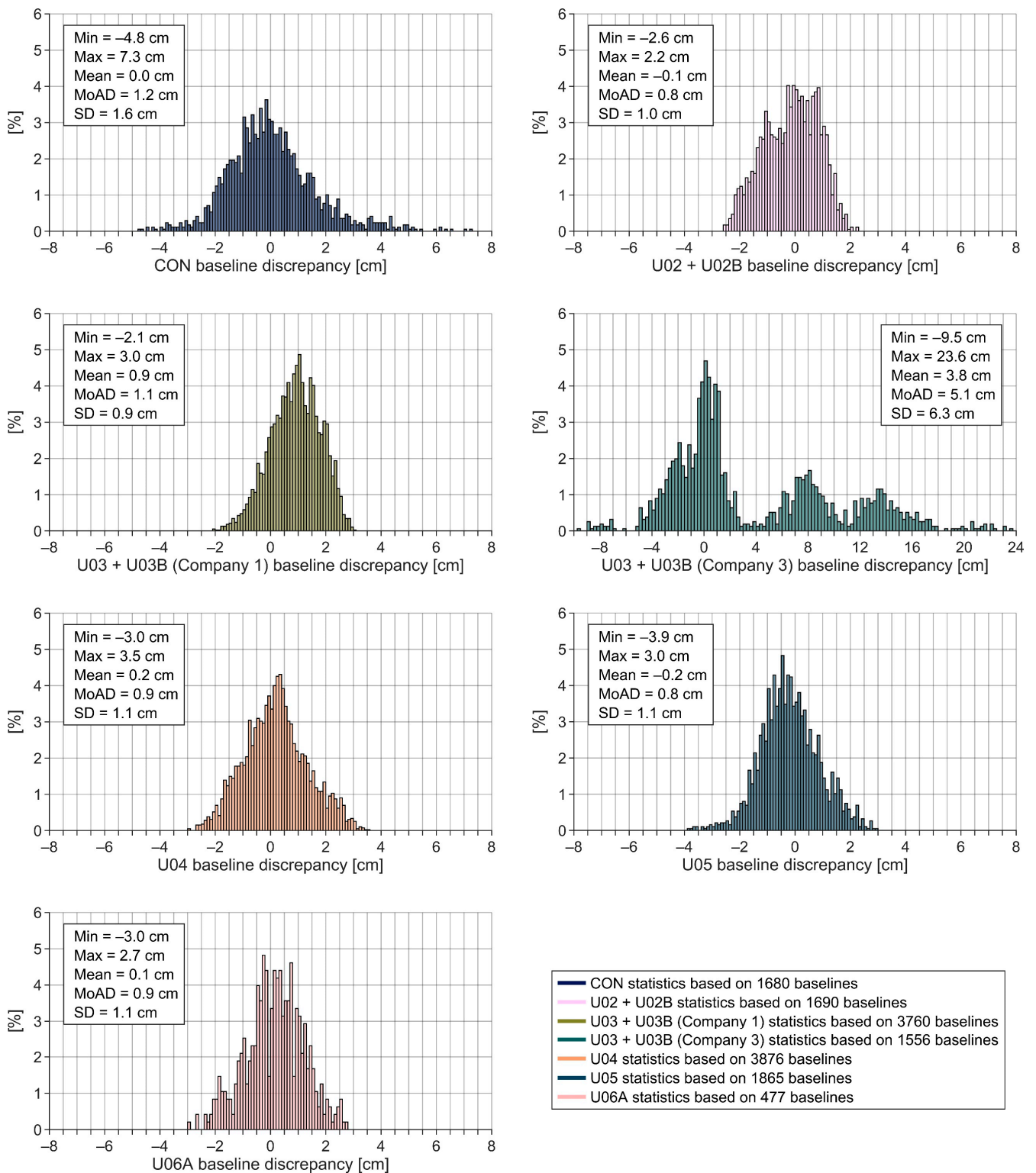
Figure 8. Histograms and descriptive statistics (MoAD—mean of absolute discrepancies; SD—standard deviation) of baseline discrepancies (cf. Equation (1)). Note that the CON-associated statistics represent an indoor survey, whereas all others describe outdoor surveys' results.
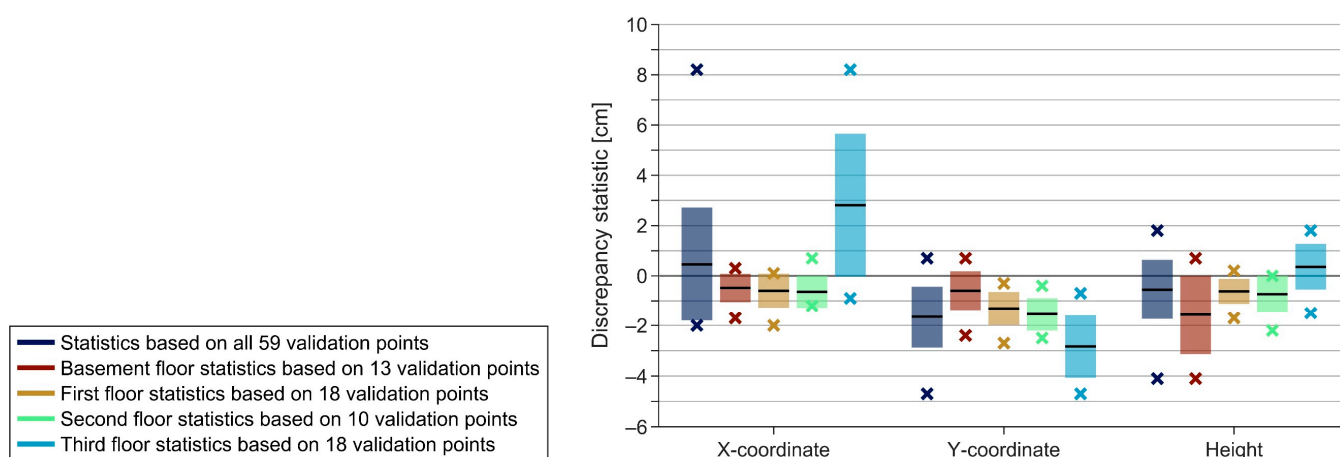
Figure 9. Descriptive statistics of discrepancies between validation points' coordinates and those extracted from each CON point cloud floor; the statistics of all 59 validation points are the same as in Figure 7. Black lines denote mean values, colored bars standard deviation estimates, and colored crosses minimum and maximum discrepancies. Notice that more significant discrepancies are associated with the basement floor (height) and third floor (*X*- and *Y*-coordinates).

The discrepancies were further examined by projecting these along a baseline aligned with the corridor connecting the secondary stairway to the main stairway (rough locations of stairways are shown in Figure A1). Figure 10 sub-plots a to c show the basement floor discrepancies and corresponding trend lines fitted in the least-squares sense. While the *X*- and *Y*-coordinate discrepancy trends reveal nothing unusual, there is a clear linear trend in height discrepancies from one stairway to the other. According to the results, a height bias of around 4 cm can be found near the secondary stairway, which evens out near the main stairway. Total station survey controls near the secondary stairway (a resection traverse loop) and main stairway (determined from outside through an open door) both provide a height error of 0.2 cm. Hence, it can be safely assumed that the discovered error of around 4 cm is due to a mistake in point cloud registration. Most alarmingly, this error could not be detected during careful visual inspection of the point cloud discussed in Section 3.

Similar discrepancy plots for the third floor are presented in Figure 10 sub-plots d to f. Again, clear discrepancy trends can be noticed from one stairway to the other, where biases appear near the secondary stairway. The most significant is a bias of around 8 cm in the *X*-coordinate, which corresponds to the roughly 7 cm registration error found during visual inspection, also mentioned in Section 3. It should be noted that a total station control measurement on survey network point D21U (cf. Figure A1) from the third-floor balcony (near the secondary stairway) provided a 0.9 cm discrepancy for the *X*-coordinate, 1.6 cm for the *Y*-coordinate, and 0.2 cm for the height, confirming that errors in the total station survey can be ruled out for the appearance of this significant bias. The 1.6 cm control discrepancy of the *Y*-coordinate (i.e., the validation survey is positively biased on the third floor, as the initial coordinates were subtracted from control measurements) explains why point cloud *Y*-coordinate discrepancies in Figure 10e have a persistent negative bias (recall that validation survey results were subtracted from the point cloud coordinates). According to the trend, the bias near the main stairway is −1.7 cm.
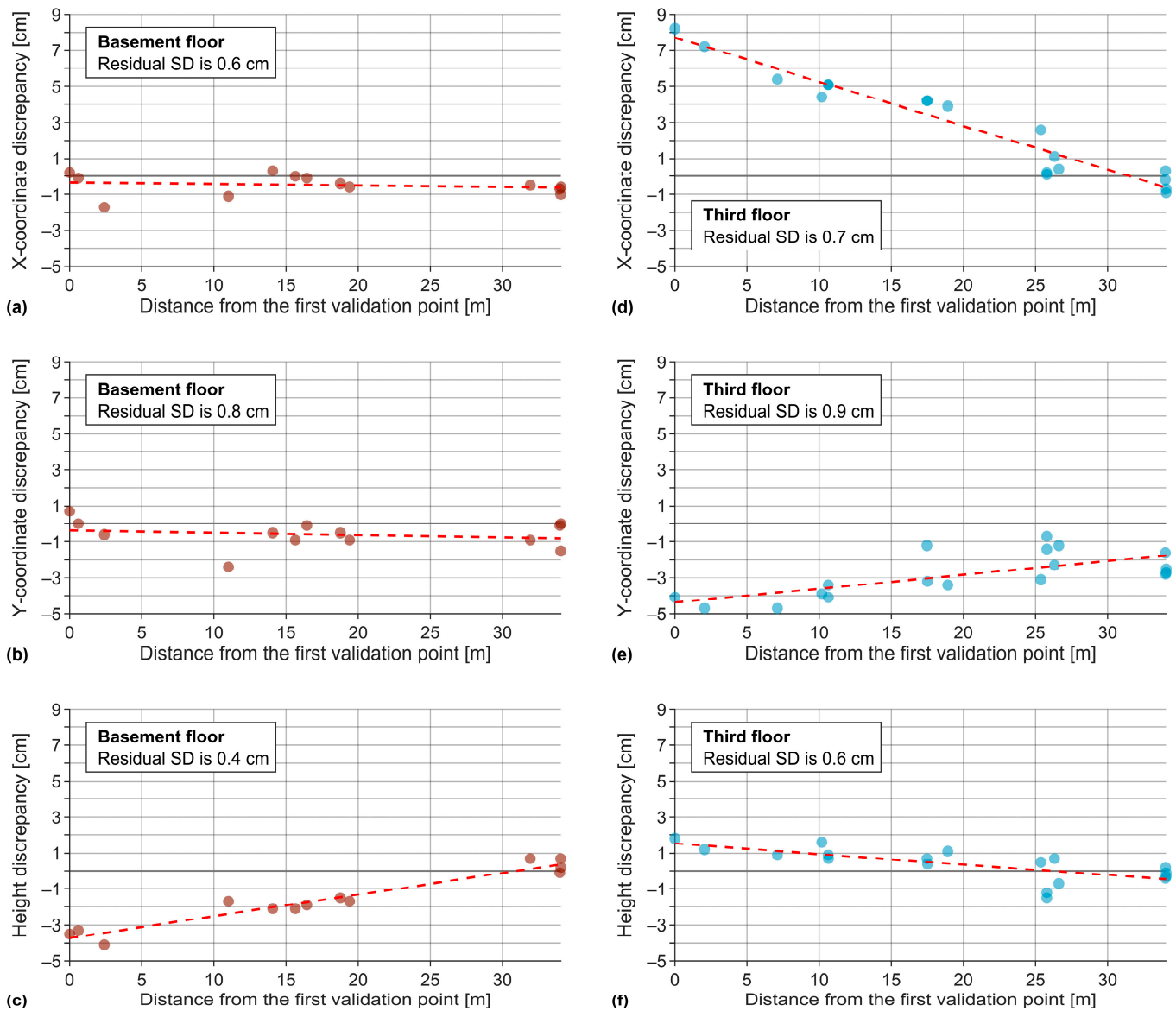
Figure 10. Discrepancies between validation points' coordinates and those extracted from the CON point cloud portion of the basement floor (sub-plots (**a**–**c**)) and the third floor (sub-plots (**d**–**f**)). The dashed red lines show the corresponding discrepancy trends. Note that discrepancies have been projected along a baseline aligned with the corridor connecting the secondary stairway (left) to the main stairway (right; refer to Figure A1). Residual standard deviation (SD) describes discrepancy residuals relative to the trend.

4.2. Point Clouds of the Main Campus Buildings

Descriptive statistics regarding discrepancies between outdoor validation points' coordinates and those extracted from the point clouds surveyed by Company 1 (U02 + U02B, U03 + U03B, U05) and Company 2 (U04 and U06A) are summarized in Figure 7 (considering all outdoor validation points). Recall that it was specified in the survey requirements provided to these surveying companies that 3 cm georeferencing accuracy must be achieved for the *X*- and *Y*-coordinates and heights relative to L-EST97 and EH2000, respectively. This requirement was imposed because point clouds (and subsequent BIM results) surveyed by different companies must be in a consistent coordinate system. Since the mean discrepancies are well within ±3 cm limits, it can be assumed that the required accuracy has been achieved for point cloud georeferencing. The largest deviation of 2.2 cm was found for

the U05 point cloud's *X*-coordinates. Most notably, the relative georeferencing accuracy of 1 cm between individual point clouds has almost always been fulfilled.

The point clouds surveyed by Companies 1 and 2 have good consistency according to Figure 7—the largest standard deviation estimate of 1.1 cm is associated with the U05 point cloud's *Y*-coordinates. Good consistency is also evident from baseline discrepancies, which yield standard deviation estimates around a centimeter for all point clouds surveyed by Companies 1 and 2 (Figure 8). Contributing factors to these estimates are point cloud registration errors, noise generated by atmospheric and environmental conditions, performance characteristics of laser scanners, beam incidence angle, and materials of surveyed surfaces [49,50], errors in the total station validation survey, and possible mismatches between validation points and the point cloud. The good quality of point clouds can be acknowledged despite all these error sources and the sheer size of point clouds, whereby the 1 cm point cloud accuracy requirement can be considered fulfilled (at least based on the outdoor validation; recall the notion at the end of Section 3 that more significant visually detectable registration errors were more likely to appear outdoors than inside the buildings).

Compared to the point clouds surveyed by Companies 1 and 2, the U03 + U03B C3 point cloud quality is worse (this was also clear from visual inspections discussed in Section 3). On the one hand, this has to do with more loose accuracy requirements, but then again, some of the revealed errors seem to be due to negligence. As indicated in Section 2.3, inaccurate georeferencing was expected, which is now confirmed with the validation survey (e.g., the 13.0 cm mean height discrepancy in Figure 7). The registration errors have also been quantified, resulting in standard deviation estimates of 4.8 cm for the *X*- and *Y*-coordinates and 1.6 cm for the height (cf. Figure 7). Comparison between baselines yields a 6.3 cm standard deviation estimate, whereby the maximum baseline discrepancies are up to 23.6 cm (cf. Figure 8). It must be stressed that the same validation points used for assessing the U03 + U03B C3 point cloud were employed to validate the U03 + U03B C1 point cloud (i.e., the quantified errors in Company 3's results are most certainly associated with the point cloud).

It can be noticed in Figure 8 that the U03 + U03B C1 point cloud has its baseline discrepancies positively skewed, which could indicate an error in the point cloud scale (another possibility is accumulating registration errors). The scale error *SE* was estimated as:

$$SE = \frac{1}{N} \sum_{i=1}^{N} \frac{D_i^{Baseline}}{TS_i^{Baseline}}, \tag{2}$$

where *N* is the total number (3760 in this case) of determined baselines (also refer to Equation (1)). The baseline discrepancies were also plotted relative to the estimated baseline lengths from total station surveys for further analysis (cf. Figure 11a). A trend line was then fitted in the least-squares sense to the plotted discrepancies, and a Pearson correlation coefficient was calculated. Based on the U03 + U03B outdoor total station validation survey, the scale error suggests an artificial lengthening of 2.7 mm per 10 m for the Company 1 surveyed point cloud. On the other hand, although there appears to be a mild trend in the data (the trend-based scale error is 0.6 mm per 10 m), the baseline discrepancies are only weakly correlated with the baseline lengths. Based on these results, conclusive evidence for erroneous scaling cannot be drawn. Because the Company 3 point cloud is validated using the same total station measurements, a similar analysis was conducted for comparison (cf. Figure 11b). Unfortunately, significant point cloud errors dominate these results.
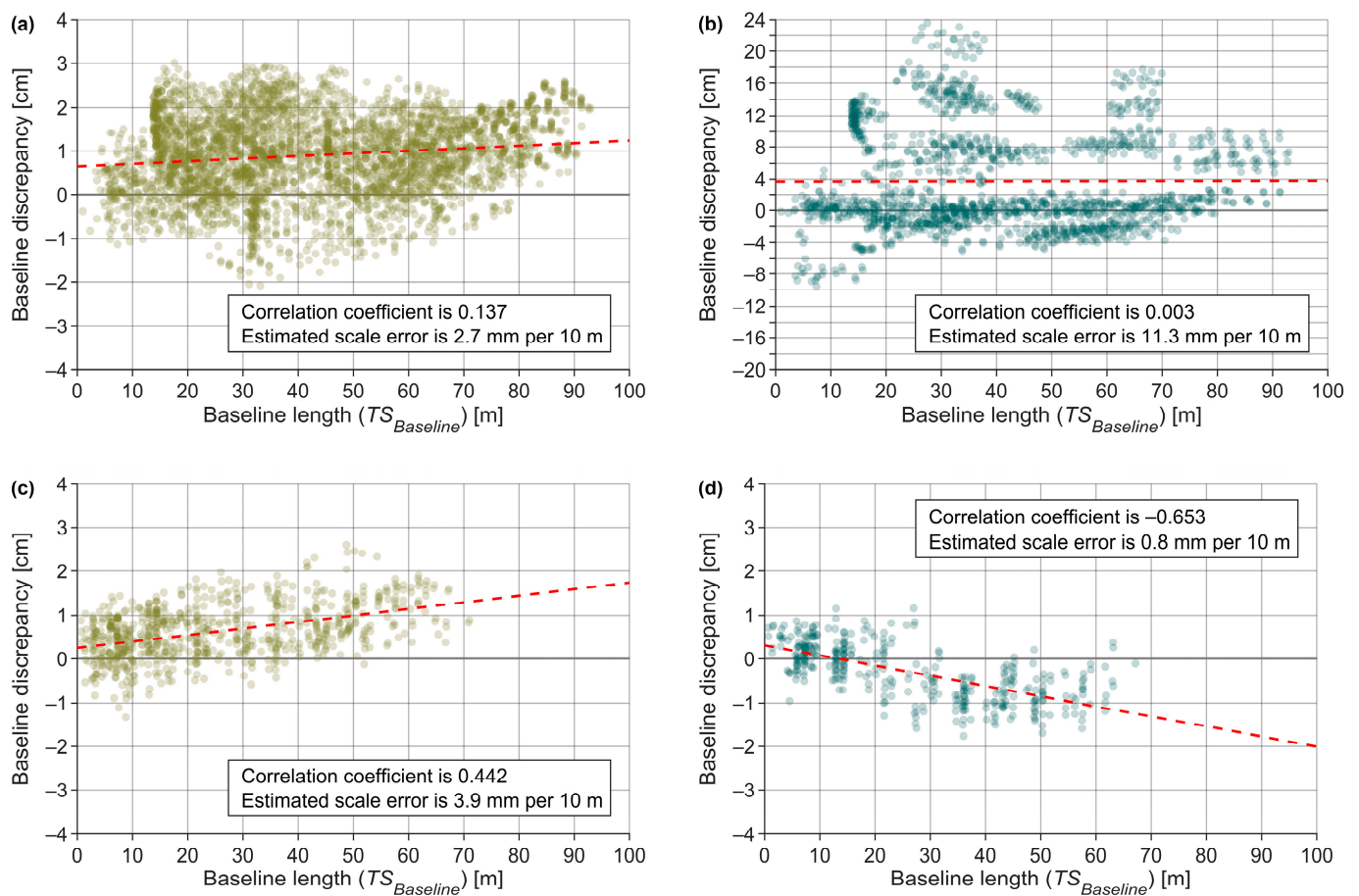
Figure 11. Baseline discrepancies (the same as in Figure 8) plotted relative to the total station estimated baseline lengths for U03 C1 (**a**) and U03 C3 (**b**) outdoor and U03 C1 (**c**) and U03 C3 (**d**) third-floor surveys. The dashed red lines show the corresponding trends, and the scale error values are estimated according to Equation (2).

Point Clouds of the U03 Building's Third Floor

Descriptive statistics regarding discrepancies between validation points' coordinates and those extracted from the point clouds of the U03 building's third floor are summarized in Figure 12. It can be noticed that the Company 1 point cloud validation results agree relatively well with those shown in Figure 7. On the other hand, the Company 3 point cloud results are biased. For example, Figure 7 provides a mean discrepancy of 13.0 cm for the height, while Figure 12 shows an 18.1 cm mean height discrepancy. In other words, due to registration errors, the point cloud portion representing the third floor has shifted relative to the general structure representing the outer walls (there are also significant registration errors in the outer wall point cloud affecting the mean discrepancies, as was shown in Section 4.2). Similar magnitude biases are also seen in the *X*-coordinate (−5.6 cm and −1.7 cm, respectively) and *Y*-coordinate's (3.1 cm and 7.8 cm, respectively) mean discrepancies.

Regarding the investigation of baseline discrepancies, both point clouds appear to show excellent consistency with the validation survey—the standard deviation estimates are 0.6 cm (cf. Figure 13). It can also be noticed that, similarly to the outdoor validation results, the baseline discrepancies of Company 1's point cloud are positively skewed, again suggesting point cloud scale error. Using Equation (2), the estimated artificial lengthening of the point cloud is 3.9 mm per 10 m, which is somewhat larger than the previous estimate of 2.7 mm per 10 m. The baseline discrepancies are now moderately correlated with the baseline lengths, and the trend in data is more evident (cf. Figure 11c); the trend-based

scale error is smaller, being 1.5 mm per 10 m. Note that the indoor and outdoor total station validation surveys are entirely independent (see Appendix A.4).
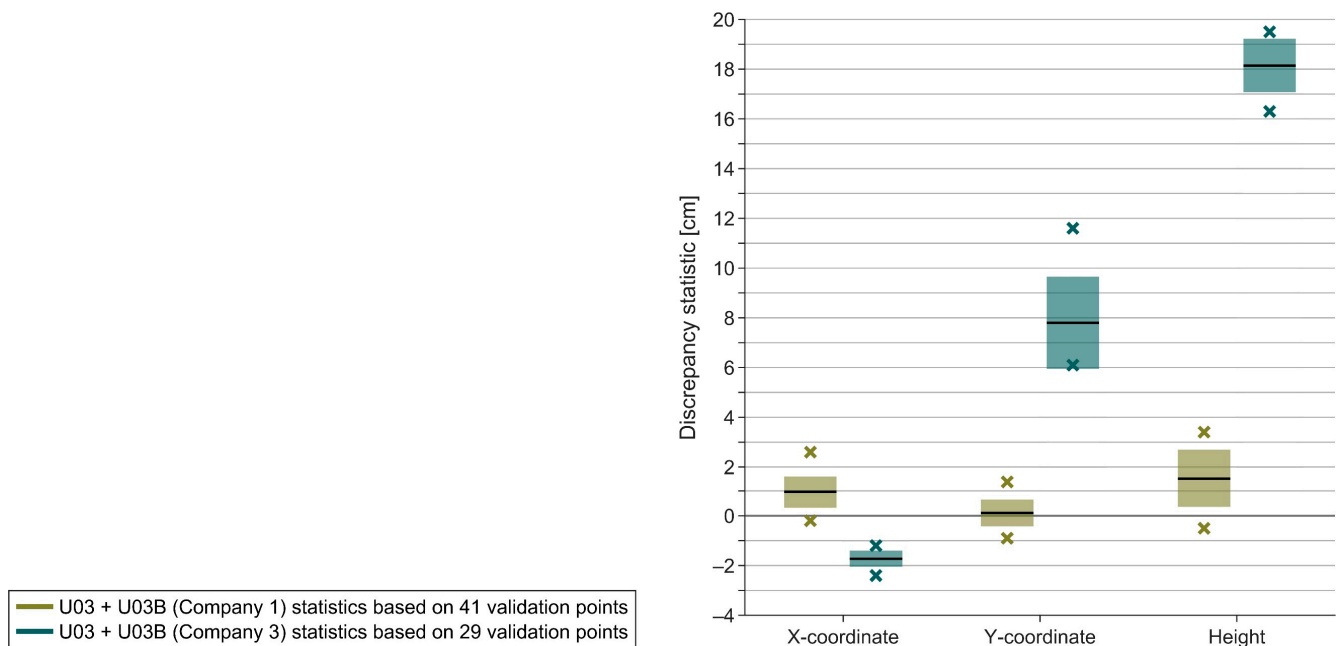

Figure 12. Descriptive statistics of discrepancies between validation points' coordinates and those extracted from the point clouds of the U03 building's third floor. Black lines denote mean values, colored bars standard deviation estimates, and colored crosses minimum and maximum discrepancies.
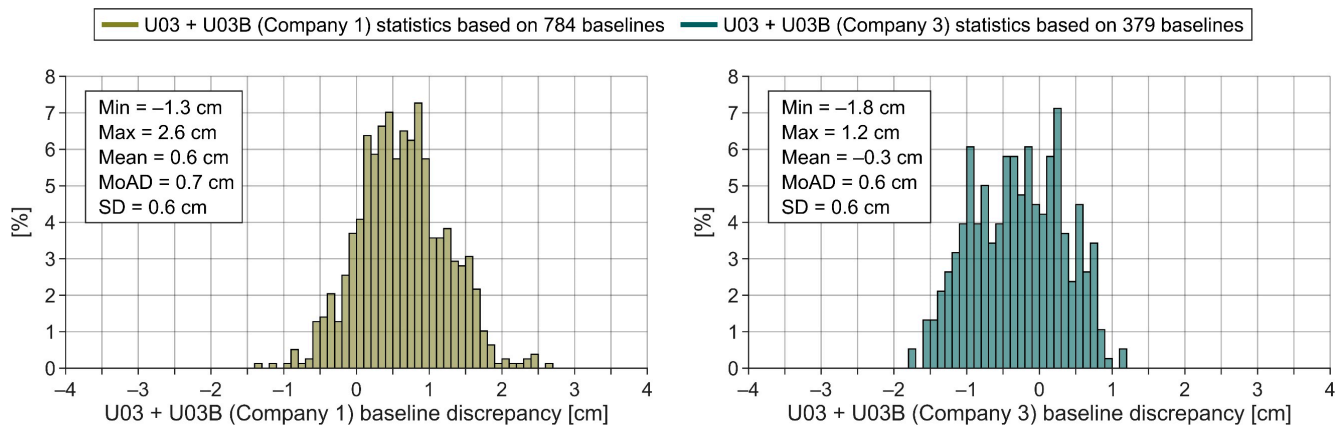

Figure 13. Histograms and descriptive statistics (MoAD—mean of absolute discrepancies; SD—standard deviation) of baseline discrepancies (cf. Equation (1)) representing the U03 building's third floor.

Although baseline discrepancies suggest that the point clouds' portions of the U03 building's third floor are consistent, the baseline-based assessment is blind to biases and tilts in the point cloud. Therefore, point cloud discrepancies relative to validation points were projected along a baseline aligned with the corridor connecting the secondary stairway to the main stairway (locations of stairways are shown in Figure A3) for further investigation. Figure 14 sub-plots b and c reveal clear linear trends (fitted in the least-squares sense) of discrepancies for the Company 1 point cloud *Y*-coordinates and height, respectively (*X*-coordinate trend is discussed in the next paragraph). The results suggest that point cloud registration has been successful at the secondary stairway, but a mistake has been made in the main stairway's registration. The most significant is a roughly 4 cm bias in height, which remained hidden from visual inspection of the point cloud discussed in Section 3.

However, residual standard deviation estimates (after removing trends from the initial discrepancies) from 0.3 cm to 0.4 cm demonstrate that the point cloud is highly consistent despite the biases. This result demonstrates that, in principle, sub-centimeter point cloud accuracy can be achieved for a point cloud portion representing a single building story.
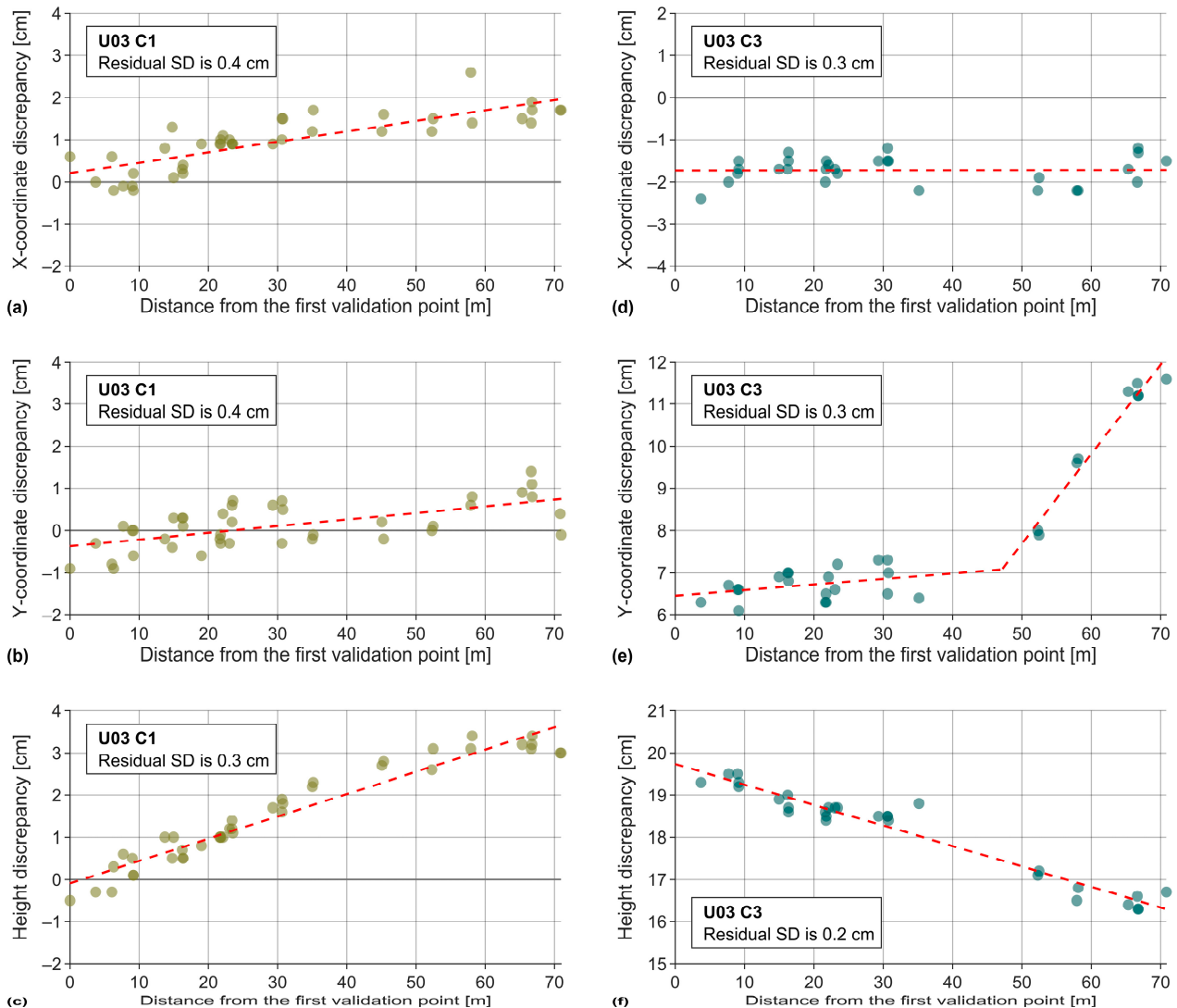

Figure 14. Discrepancies between validation points' coordinates and those extracted from the U03 C1 (sub-plots (**a**–**c**)) and U03 C3 (sub-plots (**d**–**f**)) point clouds. The dashed red lines show the corresponding discrepancy trends. Note that discrepancies have been projected along a baseline aligned with the corridor connecting the secondary stairway (left) to the main stairway (right; refer to Figure A3). Residual standard deviation (SD) describes discrepancy residuals relative to the trend. Notice vertical scale offsets in the C3-associated sub-plots.

A curious observation in Figure 14a is that the trend associated with the *X*-coordinate discrepancies is larger than that of the *Y*-coordinate. Because the corridor connecting stairways is roughly aligned with the *X*-coordinate axis (cf. Figure A3), such a result makes little sense unless it is due to a scale error. Hence, Figure 14a appears to support the speculation that the scaling of the U03 + U03B C1 point cloud is erroneous. In this case, the trend-based (Figure 14a) scale error is estimated at 2.5 mm per 10 m. Accumulating registration errors are unlikely, considering the point cloud's high consistency (residual standard deviation estimates are from 0.3 cm to 0.4 cm).

A similar analysis was conducted for Company 3's surveyed point cloud (see Figure 14 sub-plots d to f). As should be expected, the trend in X-coordinate discrepancies is not tilted. Compared to the Company 1 point cloud, the trend in height discrepancies is now tilted in the opposite direction. However, the magnitude remains similar—around 4 cm from one stairway to the other. Most interestingly, one linear trend is insufficient for describing the Y-coordinate discrepancies. At around two-thirds distance from the secondary stairway, there is a bend in the point cloud with an angle of around 6.9′, hidden from visual inspection. This bend in the point cloud explains the negative correlation in Figure 11d (i.e., due to the slight bend, the baselines determined from the point cloud shorten), the spread of Y-coordinate discrepancies in Figure 12, and the slightly negative mean baseline discrepancy in Figure 13. Although residual standard deviation estimates are from 0.2 cm to 0.3 cm (i.e., an excellent agreement between the point cloud and validation survey), the point cloud cannot be considered consistent due to the bend.

5. Discussion

Examinations of surveying-industry-produced point clouds have revealed commonly occurring significant registration errors (see Figure 6 for a visualization). For instance, on the third floor of the CON building point cloud, an error of around 7–8 cm was determined (discussed in Section 4.1). If these errors can be found visually, they can be (in principle) corrected while compiling the compound point cloud. However, a rather alarming outcome of the study is that significant registration errors may remain hidden during visual inspection. Only with a validation survey was it possible to determine that the CON (cf. Figure 10c) and U03 C1 (cf. Figure 14c) point clouds contain around 4 cm height errors. In addition, an unrealistic bend with an angle of around 6.9′ was found in the U03 C3 point cloud (cf. Figure 14e; also, a trend in height is visible from Figure 14f). A common characteristic for these hidden errors seems to be that these appear in the vicinity of complex element combinations, such as stairways (the 7–8 cm error in the CON point cloud is also associated with a nearby stairway). One potential cause for such errors could be that incorrect local optimal point cloud registration solutions (i.e., point cloud portions match in a smaller local region, but there may still exist shifts or tilts between them) have been assumed true [51]—a drawback of the iterative closest point method (i.e., the basis for point cloud registration implemented in Leica Cyclone Core and FARO Scene). Thus, it appears that the registration of point cloud portions of individual stories via stairways requires meticulous attention. The initial proper alignment of point cloud portions prior to registration is crucial [52].

Such systematic errors in point clouds, which propagate to BIM models based on these point clouds, can be consequential. Without proper knowledge of point cloud errors, systematic tilts and offsets in the compound point cloud structure could be interpreted (through comparisons with an as-designed digital model or by examining the point cloud itself) as, for example, construction errors and problems with structural integrity. Depending on their magnitude and interpretation, point cloud errors may lead to financial implications. For instance, if a hazard to a building is suspected, there might be a need to launch further investigations, such as deformation monitoring, to determine the cause of discrepancies, which, in reality, originate from point cloud errors. Alternatively, prefabricated construction element (e.g., a flight of stairs) dimensions, designed according to a digital model, may not fit the designated location during renovation or reconstruction. In other words, a BIM model that provides the basis for designing dimensions may not represent the actual building under consideration due to geometric errors. For example, some geometric accuracy requirements are defined in the New Zealand BIM handbook [53]. Accurate geometry is also necessary for other purposes like building energy performance [54–56] and load-bearing or structural analysis [57–59] computations, where systematic errors in point clouds (and, consequently, in BIM models) can lead to distorted results. During construction, automated quality controls [4,60] could also be falsely triggered.

It should be highlighted here that point clouds are not validated in industry practice. At most, point clouds are examined visually (these are also often neglected, which

is the likely case with the Company 3 provided point cloud). However, visual inspection may not reveal all the errors. One of the reasons for neglecting validations is that the above-described visual inspections and validation surveys are rather effort-consuming. Industry practitioners might also unknowingly assume the flawlessness of the used software. Although it should be admitted that other companies may obtain different results than those presented and that the varying expertise of practitioners influences the point cloud quality differently, the examinations of this study found similar significant errors in most point clouds, suggesting that malpractice is systematic. A solution could be to employ as-designed models if these are available. Although point clouds are usually employed to compare built geometry to an as-designed digital model and adjust the latter, an as-designed model could similarly be used for detecting significant point cloud errors. For instance, obvious tilts and corridor bends, as were discussed, could likely be identified and then corrected during point cloud compilation; according to the results, these errors appear systematic. Applying such an automated control could be essential for finding errors hidden from visual inspection. The implementation of an automated point cloud control using as-designed digital models should be investigated in future studies.

The validation surveys also indicate that the U03 + U03B C1 point cloud might have an erroneous scale. Various scale error estimates were obtained, but it seems that the error magnitude could be around 2 to 3 mm per 10 m. It is possible that a practitioner made a mistake during point cloud data processing. If the aim of the point cloud is to provide exact geometric information, such systematic scale errors must not be allowed. The baseline comparison approach utilized in this study provides a control for the point cloud scale and should be adopted by the surveyors. A convenient way to verify the scale is to use the same points employed in georeferencing—the baseline lengths between points from the georeferencing survey must match those determined using the point cloud. If a scale error is present, the point cloud scale can be adjusted, for example, using the open-source software CloudCompare.

Despite the flaws in point cloud registration and hidden errors around the 5 cm range, the quality of the CON point cloud and point clouds surveyed by Companies 1 and 2 can be considered, in general, good. Unfortunately, the same cannot be said about the U03 + U03B C3 point cloud. Although the expected accuracy for this survey was lower compared to those of Companies 1 and 2, some of the point cloud flaws appear to be due to negligence. As such, significant registration errors were found and quantified (e.g., baseline discrepancies up to 23.6 cm in Figure 8). This outcome illustrates that there must be some inspection from the client's side. If such a point cloud is used for constructing a BIM model (imagine a case where the client is not interested in receiving the point cloud but only the model), then, obviously, the model is similarly incorrect and does not represent the actual geometry of a building. However, it ought to be emphasized that the Company 3 surveyed point cloud was not meant to be used in a scan-to-BIM workflow.

Conversely, one of the applications of point clouds surveyed by Companies 1 and 2 is the compilation of BIM models—there is an aim to digitize the entire Tallinn University of Technology campus. This study focused on the achievable quality and accuracy of point clouds, but the correspondence of BIM models to the surveyed point clouds is similarly important. Such a study has been conducted by Esfahani et al. [61], who demonstrated that in a manual modeling scenario, the discrepancies can reach several centimeters and that semi-automated scan-to-BIM workflows should be preferred. Since the errors in a point cloud and the BIM model compiled based on it are cumulative, the final digital model can deviate significantly from the actual building geometry. Hence, following the results of this study and that of Esfahani et al. [61], there is a need to implement a validation phase, which must ensure the accuracy of the input point cloud (e.g., using an as-designed digital model as mentioned above), within the usual scan-to-BIM workflow (i.e., scan–validate–BIM), especially in industry practice where errors are likely to appear.

Finally, because there is no legislation enforcing building documentation surveying accuracy in Estonia (hence the specifically designed requirements discussed in Section 2),

guidance was sought from other countries' guidelines, such as the United States Institute of Building Documentation (USIBD)-developed level of accuracy (LOA) guidelines [62]. These guidelines are partially based on the DIN 18710 engineering surveying standard (used in Europe) and follow a similar framework to the level of development (LOD) specifications used in BIM. The USIBD accuracy requirements apply both to surveying and subsequent modeling. As the digitization effort of the Tallinn University of Technology campus aims to model construction elements, LOA30 should be aimed at, which is specified at least 1.5 cm (95% confidence level, i.e., two standard deviations) or better. This specification is more rigid than the 1 cm accuracy (in terms of standard deviation) requirement imposed on Companies 1 and 2. Due to the identified systematic registration errors (around 5 cm) in the surveying-industry-produced point clouds, such a requirement is unattainable (in terms of absolute accuracy), again emphasizing that the usual scan-to-BIM workflows require a point cloud validation phase.

Recommendations for Terrestrial Laser Scanning Surveys and Data Processing

This section summarizes TLS survey requirements that are found feasible and provides some recommendations for surveys and data processing based on the study results. The survey requirements, meant for point clouds employed in a scan-to-BIM workflow, are slightly adjusted from those imposed on Companies 1 and 2, who, in general, achieved good results.

1. A generalized point cloud accuracy requirement of 1 cm (or looser) is feasible, especially for smaller point cloud portions (e.g., a single building story). However, the point clouds must be carefully checked for significant registration errors; visual validation should not be neglected. Hidden systematic errors may exist in point clouds.
2. The point cloud density requirement should be 0.5 cm (i.e., the point cloud grid resolution on a measured surface) to distinguish minor building elements.
3. The selection of TLS station locations should aim at avoiding substantial occlusions.
4. Meticulous attention should be given to the point cloud registration of complex surface geometries, such as stairways. We recommend first merging the point clouds of scanning stations belonging to a single building story. Then, the stories should be merged via stairways, and finally, the indoor point cloud structure should be merged with the outdoor portion using doorways (or other openings). The initial proper alignment of point cloud portions prior to registration is crucial.
5. Total station surveys using the resection method can provide sufficient accuracy for georeferencing terrestrial laser scanning point clouds with an accuracy of a few centimeters (a roughly 2–3 cm requirement is feasible) if resection traverses are limited to roughly 500 m (longer traverses could not be investigated in this study). Around six to eight evenly distributed scanning targets seem enough for georeferencing similar size (around 2000 m^2 footprint) point clouds of buildings.
6. Baselines between scanning targets should be used to verify the correct scaling of the point cloud. If a scale error is detected, the point cloud scale must be adjusted (e.g., using the open-source software CloudCompare).
7. Point clouds should be cleaned of noise (e.g., reflections, people, and other moving objects), especially if these are employed in some automated scan-to-BIM workflow. Such a requirement should be written down to avoid misunderstandings.
8. In the case of point cloud or BIM procurement, we encourage clients to inspect the provided point clouds visually (this should reveal most problems) and always request surveyed point clouds, even if the interest is only in the final as-built digital 3D model. Archived point clouds also enable identifying the origin of possible design or construction mistakes (assuming no significant systematic point cloud errors).

Following the formulated practical recommendations, a construction surveying continued training course was compiled for industry practitioners. The presented point cloud errors identified with the validation surveys surprised the practitioners, demonstrating a need for more knowledge regarding potential point cloud registration mistakes (e.g.,

the incorrect local optimal point cloud registration solutions of the iterative closest point method implemented in widely used commercial software). Due to time constraints and over-reliance on software algorithms, visual validations are often neglected in industry practice; the need for such controls was highlighted during the course (as well as the potential use of as-designed digital models for controls). We emphasize that similar collaboration between researchers and the industry, as in this study, is necessary, as this may reveal industry problems and define new essential research directions.

6. Conclusions

Although the accuracy of TLS-acquired point clouds is often considered at the sub-centimeter level in state-of-the-art research, such an estimate might be too optimistic for sizeable point clouds surveyed from hundreds of scanning stations in industry practice. The findings of this study suggest that for smaller point cloud portions (e.g., a single building story), sub-centimeter accuracy is quite realistic. However, problems may occur with larger, more complex structures. It was revealed that, besides visually detectable more significant errors, hidden errors may exist around the 5 cm range. Such significant errors are associated with registering point cloud portions of stories via stairways. It is emphasized that this procedure requires meticulous attention.

Significant point cloud errors can be determined using an independent validation survey, as was conducted in this study (i.e., total station validation surveys). However, the study highlights a need for automated point cloud control (e.g., using as-designed digital models) that could reveal problematic point cloud portions instead because point cloud validation surveys are rather effort-consuming. Such control could be a valuable phase within the usual scan-to-BIM workflow to ensure that the final model corresponds accurately to the actual building geometry. As an intermediate step, practical recommendations for TLS surveys and data processing were formulated to ensure point cloud quality. Relatedly, it is concluded that improved collaboration between researchers and the industry is required, for example, by conducting continued training courses for practitioners, as there is a need for more knowledge regarding good survey and data processing practices.

The study also examined point cloud georeferencing. It was found that georeferencing errors generally remain around 2 cm using the resection method with traverses up to around 500 m. This result confirms that common surveying techniques (i.e., the resection method) used in practice can provide high and sufficient accuracy. Relatedly, the total station validation surveys demonstrated that rigorous application of the resection method could provide a few millimeters of height accuracy for complex survey networks.

Appendix A. Technical Details of Total Station Validation Surveys

Appendix A.1. Validation Survey of the CON Point Cloud

The following principles were followed during the CON point cloud validation survey:

1. All resections were established with two full measuring rounds (i.e., face left and face right) and using a minimum of five existing points. An exception was the survey base station (notice the green triangle in Figure A1) established using points D12U and D15U (cf. Figure A1) and a third to the east, further away from the building.
2. New survey network points were established permanently using survey nails (outdoors; cf. Figure A1) or temporarily using masking tape (indoors), on which appropriate markings were drawn.
3. Point cloud validation points' locations were selected where an exact match with the point cloud could be established. The match was established either with a specific point cloud data point or one that could be easily interpolated using the point cloud. If discrepancies existed between point clouds of scanning stations in a compound point cloud, point cloud points were selected from a more dense and higher intensity point cloud group (i.e., measured from a closer scanning station) representing a validation point's location.
4. Survey nails and taped points on the floor were coordinated using a mini prism (shown in Figure A2) meant for accurate engineering surveys (a tripod was not used during the CON building survey). Taped points on walls and validation points were coordinated using reflectorless distance measurements (incidence angles, i.e., an angle between a surface normal and sight path, were generally kept under 30°). The same principles were followed when establishing new resections using existing points.
5. All new survey network and validation points were coordinated with at least three full rounds. Up to six full rounds were measured depending on the total station estimated accuracy.
6. Occasional control measurements were conducted where possible, also following the above principles. For example, some control measurements were conducted through open windows and doors or on a third-floor balcony, where new coordinates were measured for an outdoor survey nail. Other control measurements represent loop closings through corridors and stairways (e.g., a resection traverse from the first floor to the basement using the main stairway was closed by going back up through the secondary stairway). Only the most recent survey network points were used to establish resections during the control measurements. Errors were estimated by comparing new coordinates to those measured initially.

As mentioned above, the base station for the total station survey was established using three available survey network points (by the time of the validation survey, most of the survey network established earlier by Varbla et al. [12] had been destroyed, primarily due to construction work). Two of these points, D12U and D15U (cf. Figure A1), had also been employed in the CON point cloud georeferencing. After the initial resection was established, points D12U and D15U were re-coordinated, whereby the coordinate differences relative to the initial ones were within a few millimeters only, suggesting no significant biases between the point cloud georeferencing and validation coordinate systems.

A total of 24 control points could be measured to assess the accuracy of the total station validation survey: 3 on the basement floor, 10 on the first floor, 4 on the second floor, and 7 on the third floor. The results in Figure A1 suggest no significant systematic effects in the survey, and errors appear random (i.e., at most, the *Y*-coordinate mean discrepancy is –0.4 cm). An accuracy of around 1–2 cm should be expected for the *X*- and *Y*-coordinates. On the other hand, the height component should have an accuracy of a few millimeters. Therefore, the conducted total station survey should be sufficient for detecting point cloud errors of a few centimeters, especially considering the height component.
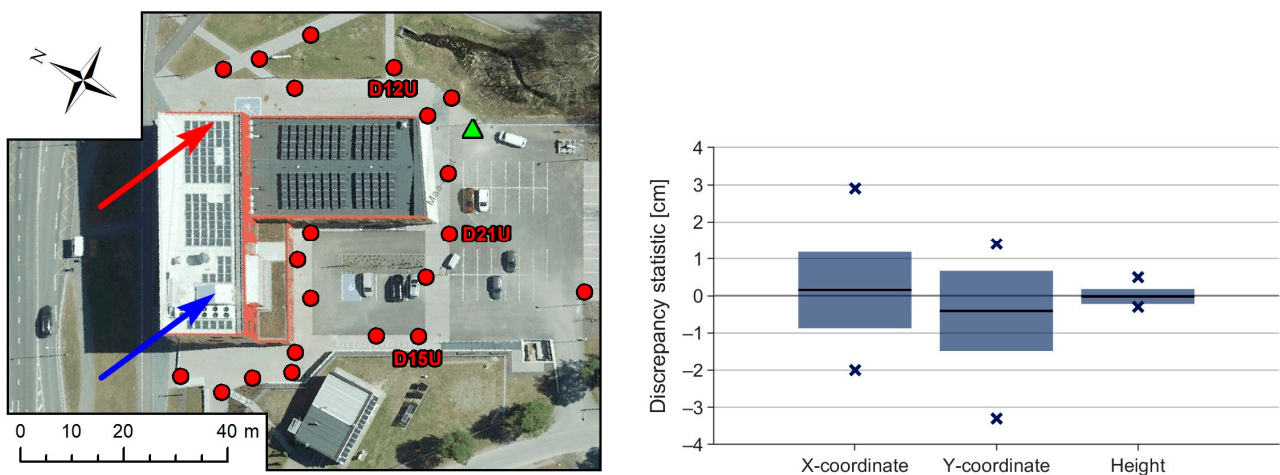
Figure A1. Outdoor survey network points (red dots) of the CON building (**left**) and descriptive statistics (based on 24 comparisons) of discrepancies between initial coordinates and control measurements (initial coordinates were subtracted from the latter) describing the CON building total station survey (**right**). On the **left** sub-plot: the green triangle shows the location of base station for the total station survey; the red arrow points roughly to the location of the main stairway, and the blue arrow points to the secondary stairway; background orthophoto originates from the Estonian Land Board. On the **right** sub-plot: black lines denote mean values, colored bars standard deviation estimates, and colored crosses minimum and maximum discrepancies.

Figure A2. Mini prism and tripod used during total station surveys.

Appendix A.2. Outdoor Survey Network for Validating Point Clouds of the Main Campus Buildings

The lessons learned during the CON building survey were considered in the subsequent total station surveys. The following principles were followed during the outdoor survey network establishment in the main campus:

1. All resections were established with two full measuring rounds and using a minimum of five (usually more) existing points.

2. New survey network points were established primarily using survey nails, but in some locations where nails could not be installed (e.g., near the trees to the north in Figure A3), screws of stable outdoor ground lamps were used instead. Out of 105 survey network points, 11 used lamp screws. One additional temporary survey network point was established with a wooden stake to support resection geometry (the yellow dot in Figure A3).

3. All survey network points were coordinated using a mini prism in combination with a tripod to maintain the levelness and stability of the prism (see Figure A2).

4. All new survey network points were coordinated with five full measuring rounds.

5. Control measurements were taken after each resection establishment on an existing survey network point to validate resection consistency with the survey network. After finalizing measurements in a station, control was repeated on the same point to validate total station stability. Each control measurement was conducted with three full measuring rounds using a mini prism and a tripod. Errors were estimated by comparing new coordinates to those measured initially.
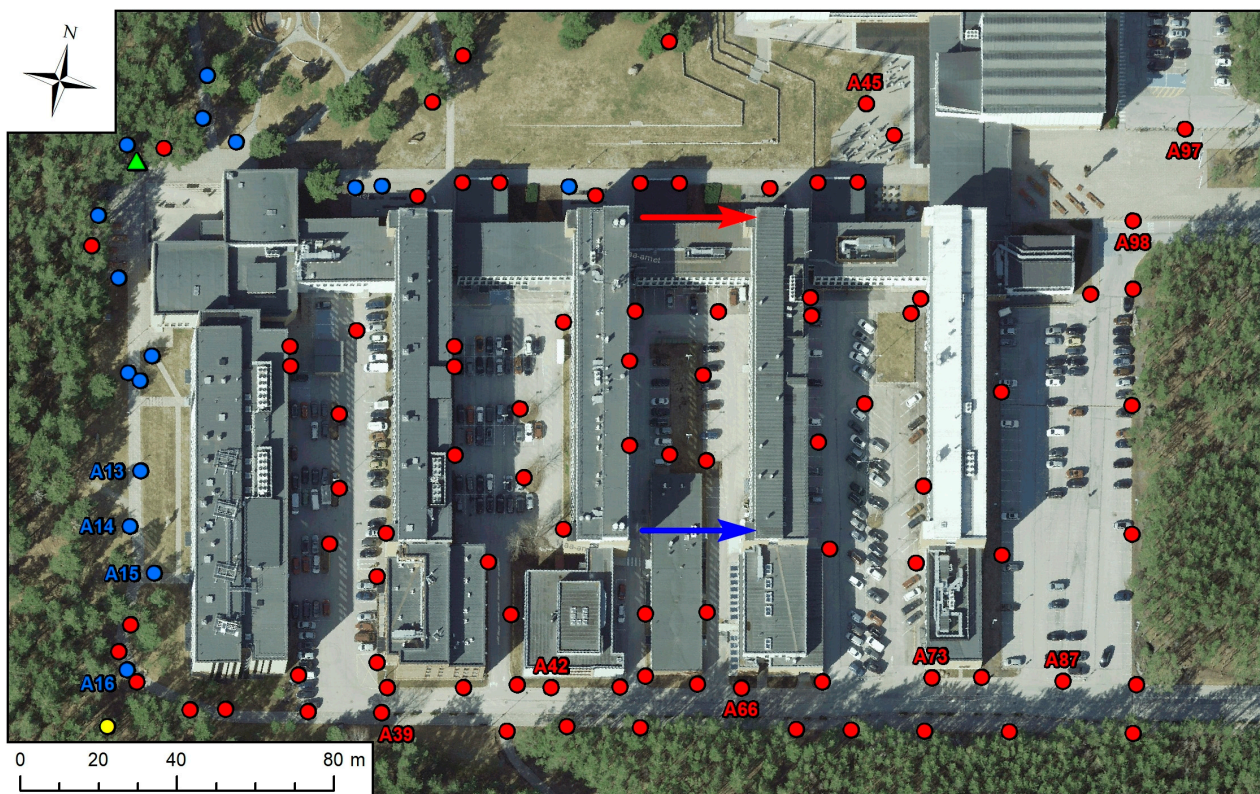

Figure A3. Outdoor survey network points (blue and red dots) for the main campus. Blue dots denote points that were initially measured using RTK-GNSS. The yellow dot denotes a temporary point established with a wooden stake, and the green triangle shows the location of the total station survey's base station. The red arrow points to the location of the main stairway, and the blue arrow points to the secondary stairway of the U03 building. Background orthophoto originates from the Estonian Land Board.

Initially, 16 survey nails were installed (notice blue dots in Figure A3), the coordinates of which were RTK-GNSS-measured relative to the Estonian national network of continuously operating GNSS reference stations [63] using a Trimble R12 GNSS receiver [64]. Ellipsoidal heights were reduced to normal heights (corresponding to the EH2000 system) using the EST-GEOID2017 [45] quasigeoid model. Each point was measured 10 times, whereby measurement cycles (point 1 to point 16) were conducted at different times (minimum time between each measurement on the same point was 30 min) on different days

(up to three cycles were measured on a single day) to allow for variations in satellite positions and numbers. Each point measurement was conducted by surveying 60 epochs with a 1 Hz frequency. Between each measurement cycle (and generally between each measurement on a consecutive survey point), the GNSS receiver was reinitialized. All these precautions were taken to minimize the appearance of systematic effects in RTK-GNSS-determined coordinates.

The final coordinates based on RTK-GNSS were determined by averaging 10 measurement results. Standard deviation estimates (based on 10 measurements) of coordinates varied from 0.6 cm to 1.6 cm for the *X*-coordinate, 0.3 cm to 1.6 cm for the *Y*-coordinate, and 0.6 cm to 2.9 cm for the height. If a total station survey's base station is established using the resection method, where the coordinates of points are determined using RTK-GNSS, Horemuž and Andersson [65] recommend using at least 10 points (minimum of 6 points). All 16 points were employed to establish this study's survey base station (notice the green triangle in Figure A3). Next, all 16 points were re-coordinated. Comparison with the initial RTK-GNSS coordinates yielded RMSE estimates (based on 16 points) of 0.7 cm for the *X*-coordinate and 0.9 cm for the *Y*-coordinate and height, demonstrating relatively good consistency of RTK-GNSS-determined coordinates. A centimeter-level accuracy should be expected for the base station position, but most importantly, these comparisons do not indicate any significant base station orientation errors.

Appendix A.2.1. Validation of the Outdoor Survey Network

Since the point clouds' validations rely on the outdoor survey network, several approaches were employed to investigate the survey network's accuracy and consistency. Keep in mind that the following validation results already consider a 0.2 cm constant shift in the *X*-coordinate, 0.6 cm in the *Y*-coordinate, and −1.5 cm in the height. These shifts of the survey network coordinates were estimated from external validations using polygonometry, precise and trigonometric leveling, and RTK-GNSS surveys, described below.

First, control-measured coordinates were compared to those determined initially (i.e., resection consistency and total station stability validation). The resulting RMSE estimates (calculated based on 56 measurements) were 0.6 cm for the *X*-coordinate, 0.5 cm for the *Y*-coordinate, and 0.1 cm for the height, suggesting good consistency of the outdoor survey network coordinates. Note that these RMSE estimates were calculated by considering both control measurements conducted after resection establishment and those after finalizing measurements in a station. Movements of the total station position (i.e., the stability) remained generally within 0.2 cm. Although this validation provides promising results, it only represents a limited area, as visibility from a survey station to a network point is required.

A more reliable validation can be conducted by closing resection traverse loops. Three such loop closings could be facilitated: two through corridors (loops 1 and 2) and one through the main entrance foyer (loop 3). The scheme of these loop closings is shown in Figure A4. Note that resections were established using only existing points on the survey stations' side relative to the buildings; survey network points used for closing the loops were not included. Discrepancies in *X*- and *Y*-coordinates in the 1–2 cm range (cf. Figure A4) suggest relatively good consistency for the outdoor survey network. What is worth highlighting is the height discrepancies of a few millimeters, demonstrating that the resection method can provide excellent height determination accuracy (the principles listed at the beginning of Appendix A.2 are a crucial factor).

Precise leveling results between two benchmarks (the U02 benchmark, cf. Figure A4, and another located to the west) could be used to validate the height accuracy. A Trimble DiNi 0.3 mm digital level [66] was employed with invar leveling staffs; survey network points were leveled using intermediate sights. Note that one millimeter was subtracted from leveled heights because survey nails have a slight depression for the prism's tip. After adjustment computations, the comparison between leveled heights and survey network heights (leveled heights were subtracted from the network heights) yielded discrepancies

of 0.1 cm for point A13, −0.5 cm for A14, and 0.0 cm for A15 and A16 (refer to Figure A3 for points' locations). A slightly larger discrepancy for point A14 could be considered an outlier (e.g., it could be that a slight pebble was under the leveling staff), as there was no indication of such an error during the total station surveys. Additionally, trigonometric leveling observations (using three full measuring rounds) were made during total station surveys on benchmarks of the U01 and U02 buildings (cf. Figure A4). The U01 benchmark height was measured once, and the U02 benchmark four times from different survey stations. Comparisons between the official height of the U02 benchmark and trigonometric leveling observations always yielded a discrepancy of 0.0 cm. For the U01 benchmark, a discrepancy of 0.3 cm was determined (official height was subtracted from the trigonometric leveling result). This more considerable discrepancy appears to be confirmed by the resection traverse loop 3 height discrepancy of 0.2 cm (cf. Figure A4).
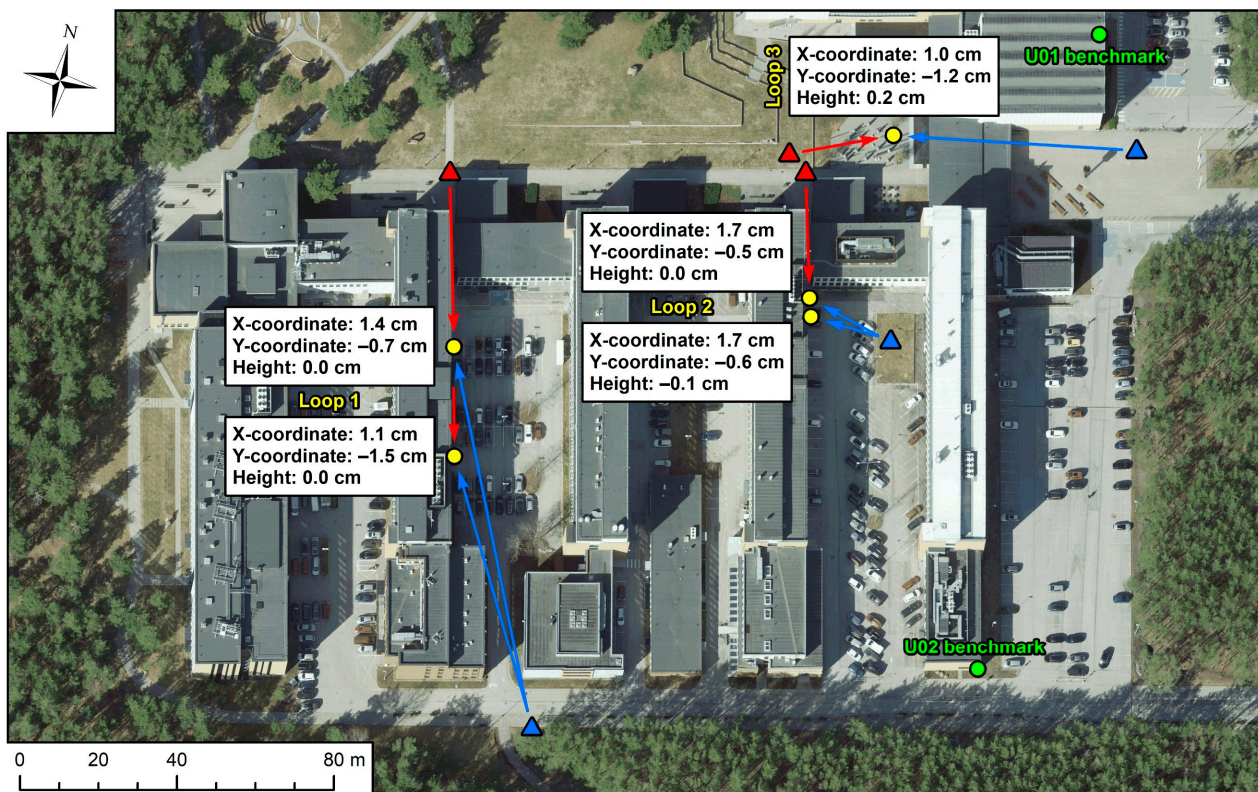

Figure A4. Scheme of resection traverse loops' closings. Yellow dots denote survey network points used for closing the loops. Red triangles and arrows show survey stations' locations and prism sights for determining the initial coordinates of survey network points, whereas blue triangles and arrows denote survey stations' locations and prism sights of control measurements. Numbers associated with *X*- and *Y*-coordinates and heights show discrepancies between initial coordinates and control measurements (initial coordinates were subtracted from the latter). Background orthophoto originates from the Estonian Land Board.

The accuracy of *X*- and *Y*-coordinates could be validated using the results of a polygonometric survey between two local geodetic network polygonometry benchmarks. A Trimble S6 2″ robotic total station [38] was employed. After adjustment computations, accurate coordinates for survey network points A16, A42, A66, A73, and A87 (refer to Figure A3) were obtained and compared to those determined by resection traverses (i.e., the outdoor survey network coordinates). The discrepancy absolute values did not exceed 0.4 cm for the *X*-coordinates and 0.6 cm for the *Y*-coordinates, indicating good agreement.

Finally, for some outdoor survey network points, coordinates were also determined by RTK-GNSS measurements using a Trimble R12 GNSS receiver [64]. The adopted RTK-GNSS

survey principles were the same as described in Appendix A.2. Compared to the previous validation approaches, RTK-GNSS provides less reliable results due to lower accuracy, but these measurements are, first and foremost, helpful in detecting orientation errors. Based on discrepancies in Table A1, there are no notable orientation errors in the outdoor survey network. Furthermore, the discrepancies also demonstrate good agreement.

Table A1. Standard deviation (SD) estimates (based on 10 measurements) of coordinates measured by RTK-GNSS and discrepancies between averaged RTK-GNSS coordinates and those of the outdoor survey network (RTK-GNSS coordinates were subtracted from the latter).

Point ID (cf. Figure A3)	Estimate	X-Coordinate [cm]	Y-Coordinate [cm]	Height [cm]
A39	RTK-GNSS SD	1.1	0.4	0.6
	Discrepancy	−0.2	−2.3	−0.2
A45	RTK-GNSS SD	0.9	0.6	0.9
	Discrepancy	−1.2	0.1	−0.3
A87	RTK-GNSS SD	0.7	1.1	1.4
	Discrepancy	0.2	−1.4	−1.6
A97	RTK-GNSS SD	1.0	1.0	1.0
	Discrepancy	0.5	0.7	−0.7
A98	RTK-GNSS SD	0.3	0.4	1.4
	Discrepancy	−0.9	0.0	0.0

Considering the results of all the employed validation approaches, the accuracy of coordinate differences between any arbitrary outdoor survey network's point pair should be at least 2 cm (likely better) for the X- and Y-coordinates. The expected accuracy of a height difference is a few millimeters for any arbitrary point pair. Evidently, there should be no significant biases in the outdoor survey network relative to the Estonian national L-EST97 rectangular plane coordinate and EH2000 height systems, respectively. The survey network is, therefore, sufficiently accurate for detecting point cloud errors of a few centimeters, especially considering the height component.

Appendix A.3. Outdoor Point Cloud Validation Surveys of the Main Campus Buildings

The following principles were followed during the outdoor validation surveys:

1. All resections were established with two full measuring rounds and using a minimum of five outdoor survey network points.
2. Point clouds' validation points' locations were selected as described in Appendix A.1, principle number 3.
3. All validation points were coordinated with at least three full rounds using reflectorless distance measurements (incidence angles were generally kept under 30°). Up to six full rounds were measured depending on the total station estimated accuracy.
4. Control measurements were conducted almost as described in Appendix A.2, principle number 5. However, the tripod was not used, and five full rounds were measured to compensate for this shortcut. The RMSE estimates (calculated based on 6 to 10 measurements, i.e., separately for each point cloud validation survey, analogously to Appendix A.2.1 estimates) did not exceed 0.6 cm for the X-coordinate, 0.5 cm for the Y-coordinate, and 0.1 cm for the height, suggesting relatively good consistency between validation surveys and the outdoor survey network.

Appendix A.4. Indoor Point Cloud Validation Survey of the U03 Building's Third Floor

The following principles were followed during the U03 building's third-floor validation survey:

1. All resections were established with two full measuring rounds and using a minimum of five (usually more) existing points. There were a few exceptions when entering some rooms, where only four existing points could be used.
2. New survey network points were established temporarily using masking tape, on which appropriate markings were drawn.
3. Point clouds' validation points' locations were selected as described in Appendix A.1, principle number 3.
4. Taped points on the floor were coordinated using a mini prism in combination with a tripod. Taped points on walls and validation points were coordinated using reflectorless distance measurements (incidence angles were generally kept under 30°). The same principles were followed when establishing new resections using existing points.
5. All new survey network points were coordinated with five full measuring rounds.
6. All validation points were coordinated with at least three full rounds. Up to six full rounds were measured depending on the total station estimated accuracy.
7. Control measurements were conducted as described in Appendix A.2, principle number 5. In some survey stations, more than one survey network point was used for controls.

The U03 building's third-floor total station validation survey was initially conducted in an arbitrary coordinate system. A baseline, consisting of multiple survey network points, was first established from a single survey station along the corridor between the main and secondary stairways (refer to the arrows in Figure A3). The baseline points were needed to maintain the survey's consistency and were the primary points for conducting control measurements. Discrepancies between initial survey network points' coordinates and control measurements yielded an RMSE estimate (calculated based on 62 measurements analogously to Appendix A.2.1 estimates) of 0.3 cm for the *X*- and *Y*-coordinates and 0.1 cm for the height, suggesting that consistency was maintained.

For transforming the validation survey from an arbitrary system to the national coordinate and height systems, outdoor survey network points were measured through open windows in different rooms. In total, 14 such measurements were conducted on various outdoor network points (some were observed multiple times). These measurements were used to compute transformation parameters using a six-parameter least-squares rigid transformation proposed by Arun et al. [67]. All surveyed validation points were then transformed to the Estonian national L-EST97 rectangular plane coordinate and EH2000 height systems, respectively, using the obtained transformation parameters. The transformation residuals at outdoor network points yielded an RMSE estimate (based on 14 measurements) of 1.3 cm for the *X*-coordinate, 1.0 cm for the *Y*-coordinate, and 0.0 cm for the height, suggesting good consistency (considering potential orientation errors that may occur due to short sight lengths in rooms) between the third-floor validation survey and the outdoor survey network.

References

1. Bosché, F.; Guillemet, A.; Turkan, Y.; Haas, C.T.; Haas, R. Tracking the built status of MEP works: Assessing the value of a scan-vs-BIM system. *J. Comput. Civ. Eng.* **2014**, *28*, 05014004. [CrossRef]
2. Mill, T.; Alt, A.; Liias, R. Combined 3D building surveying techniques—Terrestrial laser scanning (TLS) and total station surveying for BIM data management purposes. *J. Civ. Eng. Manag.* **2014**, *19*, S23–S32. [CrossRef]
3. Vincke, S.; Vergauwen, M. Vison based metric for quality control by comparing built reality to BIM. *Autom. Constr.* **2022**, *144*, 104581. [CrossRef]
4. Son, H.; Bosché, F.; Kim, C. As-built data acquisition and its use in production monitoring and automated layout of civil infrastructure: A survey. *Adv. Eng. Inform.* **2015**, *29*, 172–183. [CrossRef]
5. Dong, Z.; Liang, F.; Yang, B.; Xu, Y.; Zang, Y.; Li, J.; Wang, Y.; Dai, W.; Fan, H.; Hyyppä, J.; et al. Registration of large-scale terrestrial laser scanner point clouds: A review and benchmark. *ISPRS J. Photogramm. Remote Sens.* **2020**, *163*, 327–342. [CrossRef]
6. Wu, C.; Yuan, Y.; Tang, Y.; Tian, B. Application of terrestrial laser scanning (TLS) in the architecture, engineering and construction (AEC) industry. *Sensors* **2022**, *22*, 265. [CrossRef] [PubMed]

7.   Sammartano, G.; Spanò, A. Point clouds by SLAM-based mobile mapping systems: Accuracy and geometric content validation in multisensor survey and stand-alone acquisition. *Appl. Geomat.* **2018**, *10*, 317–339. [CrossRef]

8.   Di Stefano, F.; Torresani, A.; Farella, E.M.; Pierdicca, R.; Menna, F.; Remondino, F. 3D surveying of underground built heritage: Opportunities and challenges of mobile technologies. *Sustainability* **2021**, *13*, 13289. [CrossRef]

9.   Keitaanniemi, A.; Virtanen, J.-P.; Rönnholm, P.; Kukko, A.; Rantanen, T.; Vaaja, M.T. The combined use of SLAM laser scanning and TLS for the 3D indoor mapping. *Buildings* **2021**, *11*, 386. [CrossRef]

10. Rodriguez-Gonzalvez, P.; Gonzalez-Aguilera, D.; Lopez-Jimenez, G.; Picon-Cabrera, I. Image-based modeling of built environment from an unmanned aerial system. *Autom. Constr.* **2014**, *48*, 44–52. [CrossRef]

11. Tuttas, S.; Braun, A.; Borrmann, A.; Stilla, U. Acquisition and consecutive registration of photogrammetric point clouds for construction progress monitoring using a 4D BIM. *PFG* **2017**, *85*, 3–15. [CrossRef]

12. Varbla, S.; Puust, R.; Ellmann, A. Accuracy assessment of RTK-GNSS equipped UAV conducted as-built surveys for construction site modelling. *Surv. Rev.* **2021**, *53*, 477–492. [CrossRef]

13. Wang, Q.; Kim, M.-K.; Cheng, J.C.P.; Sohn, H. Automated quality assessment of precast concrete elements with geometry irregularities using terrestrial laser scanning. *Autom. Constr.* **2016**, *68*, 170–182. [CrossRef]

14. Mill, T.; Ellmann, A. Assessment of along-normal uncertainties for application to terrestrial laser scanning surveys of engineering structures. *Surv. Rev.* **2019**, *51*, 1–16. [CrossRef]

15. Wojtkowska, M.; Kedzierski, M.; Delis, P. Validation of terrestrial laser scanning and artificial intelligence for measuring deformations of cultural heritage structures. *Measurement* **2021**, *167*, 108291. [CrossRef]

16. Kersten, T.P.; Lindstaedt, M. Geometric accuracy investigations of terrestrial laser scanner systems in the laboratory and in the field. *Appl. Geomat.* **2022**, *14*, 421–434. [CrossRef]

17. Barbarella, M.; D'Amico, F.; De Blasiis, M.R.; Di Benedetto, A.; Fiani, M. Use of terrestrial laser scanner for rigid airport pavement management. *Sensors* **2018**, *18*, 44. [CrossRef]

18. Lõhmus, H.; Ellmann, A.; Märdla, S.; Idnurm, S. Terrestrial laser scanning for the monitoring of bridge load tests—Two case studies. *Surv. Rev.* **2018**, *50*, 270–284. [CrossRef]

19. Cao, Z.; Chen, D.; Shi, Y.; Zhang, Z.; Jin, F.; Yun, T.; Xu, S.; Kang, Z.; Zhang, L. A flexible architecture for extracting metro tunnel cross sections from terrestrial laser scanning point clouds. *Remote Sens.* **2019**, *11*, 297. [CrossRef]

20. Li, D.; Liu, J.; Feng, L.; Zhou, Y.; Liu, P.; Chen, Y.F. Terrestrial laser scanning assisted flatness quality assessment for two different types of concrete surfaces. *Measurement* **2020**, *154*, 107436. [CrossRef]

21. Yu, F.; Tong, J.; Peng, Y.; Chen, L.; Wang, S. A case study on the application of 3D scanning technology in deformation monitoring of slope stabilization structure. *Buildings* **2023**, *13*, 1589. [CrossRef]

22. Pejić, M. Design and optimisation of laser scanning for tunnels geometry inspection. *Tunn. Undergr. Space Technol.* **2013**, *37*, 199–206. [CrossRef]

23. Rocha, G.; Mateus, L. A survey of scan-to-BIM practices in the AEC industry—A quantitative analysis. *ISPRS Int. J. Geo-Inf.* **2021**, *10*, 564. [CrossRef]

24. Varbla, S.; Ellmann, A.; Puust, R. Centimetre-range deformations of built environment revealed by drone-based photogrammetry. *Autom. Constr.* **2021**, *128*, 103787. [CrossRef]

25. Jo, Y.H.; Hong, S. Three-dimensional digital documentation of cultural heritage site based on the convergence of terrestrial laser scanning and unmanned aerial vehicle photogrammetry. *ISPRS Int. J. Geo-Inf.* **2019**, *8*, 53. [CrossRef]

26. Alshawabkeh, Y.; Baik, A.; Miky, Y. Integration of laser scanner and photogrammetry for heritage BIM enhancement. *ISPRS Int. J. Geo-Inf.* **2021**, *10*, 316. [CrossRef]

27. Siwiec, J.; Lenda, G. Integration of terrestrial laser scanning and structure from motion for the assessment of industrial chimney geometry. *Measurement* **2022**, *199*, 111404. [CrossRef]

28. Moyano, J.; Justo-Estebaranz, Á.; Nieto-Julián, J.E.; Barrera, A.O.; Fernández-Alconchel, M. Evaluation of records using terrestrial laser scanner in architectural heritage for information modeling in HBIM construction: The case study of the La Anunciación church (Seville). *J. Build. Eng.* **2022**, *62*, 105190. [CrossRef]

29. Ariza-López, F.J.; Reinoso-Gordo, J.F.; García-Balboa, J.L.; Ariza-López, Í.A. Quality specification and control of a point cloud from a TLS survey using ISO 19157 standard. *Autom. Constr.* **2022**, *140*, 104353. [CrossRef]

30. Bassier, M.; Yousefzadeh, M.; Van Genechten, B. Evaluation of data acquisition techniques and workflows for Scan to BIM. In Proceedings of the Geo Business, London, UK, 27–28 May 2015; Geo Business: London, UK, 2015.

31. Cheng, L.; Chen, S.; Liu, X.; Xu, H.; Wu, Y.; Li, M.; Chen, Y. Registration of laser scanning point clouds: A review. *Sensors* **2018**, *18*, 1641. [CrossRef]

32. Li, L.; Wang, R.; Zhang, X. A tutorial review on point cloud registrations: Principle, classification, comparison, and technology challenges. *Math. Probl. Eng.* **2021**, *2021*, 9953910. [CrossRef]

33. Toomsar, U. The Development of Ehituse Mäemaja Point Cloud and Digital Twin. Master's Thesis, Tallinn University of Technology, Tallinn, Estonia, 2021. Available online: https://digikogu.taltech.ee/et/Item/d0467490-087b-4ea9-bd30-989c904c1353 (accessed on 26 July 2024). (In Estonian).

34. Leica RTC360 3D Laser Scanner. Available online: https://leica-geosystems.com/products/laser-scanners/scanners/leica-rtc360 (accessed on 26 July 2024).

35. FARO Laser Scanner Focus3D X 330. Available online: https://ats.se/pdf/faro/FARO_Laser_Scanner_Focus3D_X_330_Tech_Sheet.pdf (accessed on 26 July 2024).

36. Muralikrishnan, B. Performance evaluation of terrestrial laser scanners—A review. *Meas. Sci. Technol.* **2021**, *32*, 072001. [CrossRef] [PubMed]

37. Besl, P.J.; McKay, N.D. A method for registration of 3-D shapes. *IEEE Trans. Pattern Anal. Mach. Intell.* **1992**, *14*, 239–256. [CrossRef]

38. Trimble S6 Total Station. Available online: https://geomaticslandsurveying.com/wp-content/uploads/2018/11/Trimble-S6-total-station-Datasheet.pdf (accessed on 26 July 2024).

39. McCaw, G.T. Resection in survey. *Geogr. J.* **1918**, *52*, 105–123. [CrossRef]

40. Horemuž, M.; Jansson, P. Optimum establishment of total station. *J. Surv. Eng.* **2017**, *143*, 06016004. [CrossRef]

41. Alizadeh-Khameneh, M.A.; Horemuž, M.; Jensen, A.B.O.; Andersson, J.V. Optimal vertical placement of total station. *J. Surv. Eng.* **2018**, *144*, 06018001. [CrossRef]

42. Trimble S5 Total Station. Available online: https://geosoft.ee/wp-content/uploads/pdf/Datasheet%20-%20Trimble%20S5.pdf (accessed on 26 July 2024).

43. Leica Viva TS12 Datasheet. Available online: https://www.geotech.sk/downloads/Totalne-stanice/TS12/Leica_Viva_TS12_DAT_en.pdf (accessed on 26 July 2024).

44. GRX3 GNSS Receiver. Available online: https://eu.sokkia.com/sites/default/files/product/downloads/grx3_gnssreceiver_broch_sok-1048_revc_team_en_us_hires.pdf (accessed on 26 July 2024).

45. Ellmann, A.; Märdla, S.; Oja, T. The 5 mm geoid model for Estonia computed by the least squares modified Stokes's formula. *Surv. Rev.* **2020**, *52*, 352–372. [CrossRef]

46. Bae, S.-J.; Kim, J.-Y. Indoor clutter object removal method for an as-built building information model using a two-dimensional projection approach. *Appl. Sci.* **2023**, *13*, 9636. [CrossRef]

47. Aryan, A.; Bosché, F.; Tang, P. Planning for terrestrial laser scanning in construction: A review. *Autom. Constr.* **2021**, *125*, 103551. [CrossRef]

48. Resection Computations in Trimble Access. Available online: https://help.trimblegeospatial.com/TrimbleAccess/latest/en/PDFs/Access-Resection-Computations.pdf (accessed on 26 July 2024).

49. Soudarissanane, S.; Lindenbergh, R.; Menenti, M.; Teunissen, P. Scanning geometry: Influencing factor on the quality of terrestrial laser scanning points. *ISPRS J. Photogramm. Remote Sens.* **2011**, *66*, 389–399. [CrossRef]

50. Bolkas, D.; Martinez, A. Effect of target color and scanning geometry on terrestrial LiDAR point-cloud noise and plane fitting. *J. Appl. Geod.* **2018**, *12*, 109–127. [CrossRef]

51. Li, P.; Wang, R.; Wang, Y.; Tao, W. Evaluation of the ICP algorithm in 3D point cloud registration. *IEEE Access* **2020**, *8*, 68030–68048. [CrossRef]

52. He, Y.; Liang, B.; Yang, J.; Li, S.; He, J. An iterative closest points algorithm for registration of 3D laser scanner point clouds with geometric features. *Sensors* **2017**, *17*, 1862. [CrossRef]

53. The New Zealand BIM Handbook. Available online: https://www.biminnz.co.nz/nz-bim-handbook (accessed on 26 July 2024).

54. Depecker, P.; Menezo, C.; Virgone, J.; Lepers, S. Design of buildings shape and energetic consumption. *Build. Environ.* **2001**, *36*, 627–635. [CrossRef]

55. Hong, S. Geometric Accuracy of BIM-BEM Transformation Workflows: Bridging the State-of-the-Art and Practice. Master's Thesis, Carleton University, Ottawa, ON, Canada, 2020. [CrossRef]

56. Oraiopoulos, A.; Howard, B. On the accuracy of urban building energy modelling. *Renew. Sustain. Energy Rev.* **2022**, *158*, 111976. [CrossRef]

57. Barazzetti, L.; Banfi, F.; Brumana, R.; Gusmeroli, G.; Previtali, M.; Schiantarelli, G. Cloud-to-BIM-to-FEM: Structural simulation with accurate historic BIM from laser scans. *Simul. Model. Pract. Theory* **2015**, *57*, 71–87. [CrossRef]

58. Hasan, A.M.M.; Torky, A.A.; Rashed, Y.F. Geometrically accurate structural analysis models in BIM-centered software. *Autom. Constr.* **2019**, *104*, 299–321. [CrossRef]

59. Lu, R.; Rausch, C.; Bolpagni, M.; Brilakis, I.; Haas, C.T. Geometric accuracy of digital twins for structural health monitoring. In *Structural Integrity and Failure*; Oyguc, R., Tahmasebinia, F., Eds.; IntechOpen Limited: London, UK, 2020. [CrossRef]

60. Maalek, R.; Lichti, D.D.; Ruwanpura, J.Y. Automatic recognition of common structural elements from point clouds for automated progress monitoring and dimensional quality control in reinforced concrete construction. *Remote Sens.* **2019**, *11*, 1102. [CrossRef]

61. Esfahani, M.E.; Rausch, C.; Sharif, M.M.; Chen, Q.; Haas, C.; Adey, B.T. Quantitative investigation on the accuracy and precision of scan-to-BIM under different modelling scenarios. *Autom. Constr.* **2021**, *126*, 103686. [CrossRef]

62. USIBD Level of Accuracy (LOA) Specification Guide. Available online: https://cdn.ymaws.com/www.nysapls.org/resource/resmgr/2019_conference/handouts/hale-g_bim_loa_guide_c120_v2.pdf (accessed on 26 July 2024).

63. Metsar, J.; Kollo, K.; Ellmann, A. Modernization of the Estonian national GNSS reference station network. *Geod. Cartogr.* **2018**, *44*, 55–62. [CrossRef]

64. Trimble R12 GNSS System. Available online: https://trl.trimble.com/docushare/dsweb/Get/Document-926322/022516-481C_Trimble%20R12%20GNSS%20Receiver_DS_A4_1020_LRsec.pdf (accessed on 26 July 2024).

65. Horemuž, M.; Andersson, J.V. Analysis of the precision in free station establishment by RTK GPS. *Surv. Rev.* **2011**, *43*, 679–686. [CrossRef]

66.   Trimble Dini Digital Level. Available online: https://trl.trimble.com/docushare/dsweb/Get/Document-240688/022543-327E_
       Trimble_DiNi2007_DS_USL_0920_LRsec.pdf (accessed on 26 July 2024).
67.   Arun, K.S.; Huang, T.S.; Blostein, S.D. Least-squares fitting of two 3-D point sets. *IEEE Trans. Pattern Anal. Mach. Intell.* **1987**, *9*,
       698–700. [CrossRef]